

Ethyl 8-Fluoro-6-(3-nitrophenyl)-4H-imidazo[1,5-a][1,4]benzodiazepine-3-carboxylate as Novel, Highly Potent, and Safe Antianxiety Agent

Maurizio Anzini,^{*,†} Carlo Braile,[†] Salvatore Valenti,[†] Andrea Cappelli,[†] Salvatore Vomero,[†] Luciana Marinelli,[‡] Vittorio Limongelli,[‡] Ettore Novellino,[‡] Laura Betti,[§] Gino Giannaccini,[§] Antonio Lucacchini,[§] Carla Ghelardini,^{||} Monica Norcini,^{||} Francesco Makovec,[⊥] Gianluca Giorgi,[#] and R. Ian Fryer^{∇,○}

Dipartimento Farmaco Chimico Tecnologico and European Research Centre for Drug Discovery and Development, Università degli Studi di Siena, Via A. Moro, 53100 Siena, Italy, Dipartimento di Chimica Farmaceutica e Tossicologica, Università di Napoli "Federico II", Via D. Montesano 49, 80131 Napoli, Italy, Dipartimento di Psichiatria, Neurobiologia Farmacologia e Biotecnologie, Università di Pisa, Via Bonanno 6, 56126 Pisa, Italy, Dipartimento di Farmacologia Preclinica e Clinica "M. Aiazzi Mancini", Università degli Studi di Firenze, Viale G. Pieraccini 6, 50139 Firenze, Italy, Rottapharm S.p.A., Via Valosa di Sopra 7, 20052 Monza, Italy, Dipartimento di Chimica, Università degli Studi di Siena, Via A. Moro, 53100 Siena, Italy, Department of Chemistry, Rutgers The State University of New Jersey, 73 Warren Street, Newark, New Jersey 07102

Received March 19, 2008

Ethyl 8-fluoro-6-(4-nitrophenyl)- and ethyl 8-fluoro-6-(3-nitrophenyl)-4H-imidazo[1,5-a][1,4]benzodiazepine 3-carboxylate **6** and **7** were synthesized as central benzodiazepine receptor (CBR) ligands and tested for their ability to displace [³H]flumazenil from bovine and human cortical brain membranes. Both compounds showed high affinity for bovine and human CBR. In particular, compound **7** emerged as the most interesting compound, having a partial agonist profile in vitro while possessing useful activity in various animal models of anxiety. In accordance with its partial agonist profile, compound **7** was devoid of typical benzodiazepine side effects. The homology model of the GABA_A receptor developed by Cromer et al. was used to assess the binding modes of ligands **6** and **7**. From our docking results, the partial agonist activity elicited by compound **7** is likely to be due to the 3'-nitro substituent, which is in the appropriate position to interact with Thr193 of the γ_2 -subunit by means of a hydrogen bond.

Introduction

GABA (γ -aminobutyric acid) is the most important inhibitory neurotransmitter in the brain, being able to control the excitability of many central nervous system (CNS)^a pathways. GABA exerts its physiological effects by binding to three different receptor types in the neuronal membrane: the GABA_A, GABA_B, and GABA_C receptors. The GABA_B receptor belongs to the G-protein-coupled receptors superfamily,¹ while the GABA_A² and GABA_C³ receptors are ligand-gated chloride ion channel complexes. GABA_A receptors, which are responsible for the majority of neuronal inhibition in the mammalian CNS, mediate the actions of many pharmacologically useful agents, including benzodiazepines (BDZs), barbiturates, neuroactive steroids, anesthetics, and convulsants.^{4,5}

Electron microscopy studies of the native GABA_A receptors have shown that they are composed of five subunits arranged pseudosymmetrically around the chloride ion channel pathway, which passes through the cell membrane, and the receptor appears as a "doughnut" with a diameter of around 8 nm when viewed from the cell exterior.⁶

GABA_A receptors are generally hetero-oligomers, the subunits being selected from four principal families α , β , γ , and δ , although others including ϵ , π , ρ , and θ have been identified. At present, a total of 21 subunits ($\alpha 1$ –6, $\beta 1$ –4, $\gamma 1$ –4, δ , ϵ , π , θ and $\rho 1$ –3) have been cloned and sequenced. Each of the subunit isoforms is encoded by a single gene, although additional heterogeneity is introduced by alternative splicing in a number of cases.⁷ This plethora of subunits may suggest that there exists a vast array of GABA_A receptors subtypes, but this does not appear to be the case.

GABA_A-receptor heterogeneity is expected to provide the basis for flexibility in signal transduction and drug-induced allosteric modulation. However, the most common form of the GABA_A receptor contains α , β , and γ subunits⁸ and recombinant receptors containing these subunits mimic the biological, electrophysiological, and pharmacological properties of the native GABA_A receptors. The benzodiazepine (BZ) binding site, the so-called benzodiazepine receptor (CBR), occurs at the interface of the α and γ subunits,⁹ and although the γ_2 -subunit is essential to convey classical BDZ sites to recombinant receptors, the α -subunit variants largely determine their pharmacological profiles.¹⁰ Thus, type I ($\omega 1$) and type II ($\omega 2$) benzodiazepine receptors are formed upon coexpression of the subunits $\alpha 1\beta\gamma_2$ and $\alpha 2$ - or $\alpha 3\beta\gamma_2$, respectively,¹¹ whereas receptors containing the $\alpha 4$ - or $\alpha 6$ -subunits have very low affinities for classical benzodiazepines such as diazepam (7-chloro-1,3-dihydro-1-methyl-5-phenyl-2H-1,4-benzodiazepin-2-one).¹² In particular, from independent research studies based on gene "knock in" and "knock out" strategies,⁷ it has been

* To whom correspondence should be addressed. Phone: +39 577 234173. Fax: +39 577 234333. E-mail: anzini@unisi.it.

[†] Dipartimento Farmaco Chimico Tecnologico, Università degli Studi di Siena.

[‡] Dipartimento di Chimica Farmaceutica e Tossicologica, Università di Napoli "Federico II".

[§] Dipartimento di Psichiatria, Neurobiologia Farmacologia e Biotecnologie, Università di Pisa.

^{||} Dipartimento di Farmacologia Preclinica e Clinica "M. Aiazzi Mancini", Università degli Studi di Firenze.

[⊥] Dipartimento di Chimica, Università degli Studi di Siena.

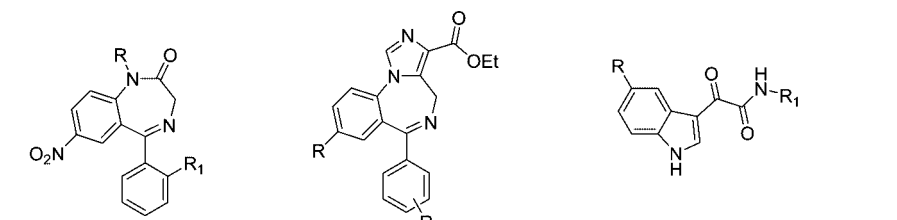
[#] Rottapharm S.p.A., Monza.

[∇] Department of Chemistry, Rutgers State University.

[○] Present address: 421 Morningwood Drive, Olney, MD 20832.

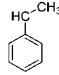
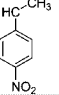
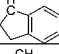
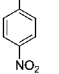
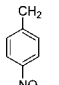
^a Abbreviations: CNS, central nervous system; CBR, central benzodiazepine receptor; BDZ, benzodiazepine; iBDZ, imidazobenzodiazepine; DPPA, diphenyl phosphorazidate; PTZ, pentylenetetrazole; MD, molecular dynamics.

Chart 1. Title and Reference Compounds



Compd	R	R ₁
1 nitrazepam	H	H
2 nimetazepam	CH ₃	H
3 clonazepam	CH ₃	Cl
4 flunitrazepam	CH ₃	F

Compd	R	R ₁
5	H	4-NO ₂
6	F	4-NO ₂
7	F	3-NO ₂

Compd	R	Config.	R ₁
8a	NO ₂	R	
8b	Cl	R	
8c	NO ₂	R	
8d	H		
8e	Cl		

evidenced that the sedative and anticonvulsant actions are mediated through α_1 -containing GABA_A receptors, while α_2 -containing receptors may be involved in anxiolytic-like activity because these have a preferential brain distribution in circuits mediating emotional behavior. Furthermore, α_2 -, α_3 -, and/or α_5 -containing receptors may mediate the muscle relaxant effect,^{7,13} even if it is now well established that α_5 -containing receptors are associated with cognition and memory while the role of α_3 -containing receptors remains unclear or, at least, they seem to be partly involved in mediating anxiety.^{14,15}

Ligands acting at the ω modulatory sites can differ by their intrinsic efficacy.¹⁶ At least three classes of compounds have been identified by their ability to modulate GABA neurotransmission by interacting with this receptor complex. Positive modulation, which leads to an increase of the GABA-induced chloride ion flux, is produced by agonists at the ω modulatory sites such as benzodiazepines [e.g., diazepam, oxazepam (7-chloro-1,3-dihydro-3-hydroxy-5-phenyl-2H-1,4-benzodiazepin-2-one), midazolam (8-chloro-6-(2-fluorophenyl)-1-methyl-4H-imidazo[1,5-a][1,4]benzodiazepine), and triazolam (8-chloro-6-(*o*-chlorophenyl)-1-methyl-4H-s-triazolo[4,3-a][1,4]benzodiazepine)],^{16,17} cyclopyrrolones [e.g., zopiclone [6-(5-chloropyridin-2-yl)-5-oxo-7H-pyrrolo[3,4-*b*]pyrazin-7-yl]-4-methylpiperazine-1-carboxylate, and suriclone [6-(7-chloro-1,8-naphthyridin-2-yl)-5-oxo-3,7-dihydro-2H-[1,4]dithiino[2,3-*c*]pyrrol-7-yl]-4-methylpiperazine-1-carboxylate],^{16,18} triazolopyridazines (e.g., 3-methyl-6-[3-(trifluoromethyl)phenyl]-1,2,4-triazolo[4,3-*b*]pyridazine (CL 218,872),¹⁷ imidazopyridines (e.g., zolpidem (*N,N*-dimethyl-2-[6-methyl-2-(4-methylphenyl)imidazo[3,2-*a*]pyridin-3-yl]acetamide),¹⁹ β -carbolines (e.g., ethyl 5-benzyloxy-4-methoxymethyl- β -carboline-3-carboxylate (ZK 91296),²⁰ imidazopyrimidines,²¹ flavones,²² and quinolines.²³ Negative modulation, which induces a decrease of the GABA-induced chloride ion flux, is obtained by inverse agonists, such as β -carbolines (e.g., β -CCM and DMCM),^{20,24} pyrazoloquinolines (e.g., 2-phenyl-2,5-dihydro-3H-pyrazolo[4,3-*c*]quinolin-3-one (CGS 8216),²⁵ whereas competitive antagonists of the ω modulatory sites (such as the imidazobenzodiazepine flumazenil,²⁶ the β -carbolines ethyl 5-isopropoxy-4-methyl- β -

carboline-3-carboxylate (ZK 93426),²⁷ PrCC,²⁸ and β -CCt²⁹) bind without intrinsic activity.

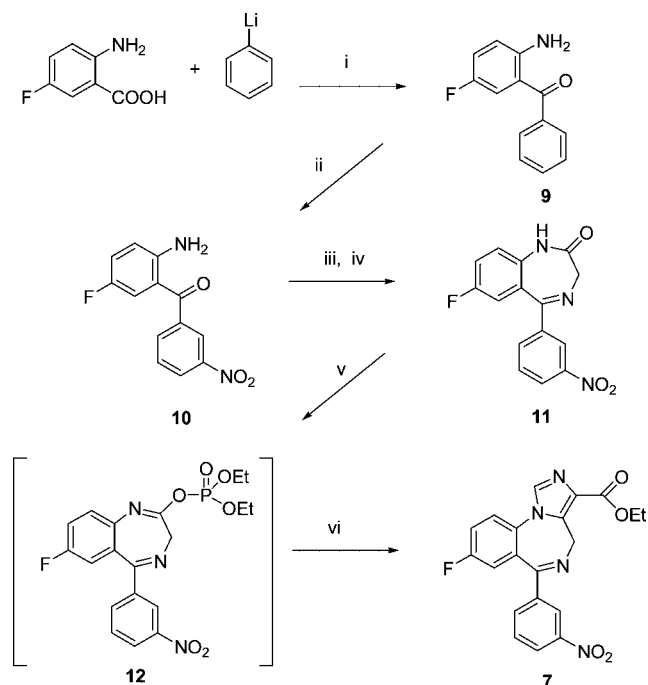
In particular, among classic 1,4-benzodiazepines, 7-nitro-derivatives as nitrazepam (**1**), nimetazepam (**2**), clonazepam (**3**), and flunitrazepam (**4**) (Chart 1) act as full agonists at central benzodiazepine receptor (CBR) and are marketed as hypnotics, anticonvulsants, and sedative/muscle relaxants, respectively, while in other classes of nitro-substituted ligands at CBR the different position of the NO₂ group present in the scaffold or in the pendant phenyl ring leads to compounds showing different intrinsic activity such as Ro 23-2896 (**5**), an imidazobenzodiazepine 4'-nitroderivative which behaves as an antagonist,³⁰ while the indol-3-yl-glyoxylamides **8a–e** proved to act as partial agonists, antagonists, or inverse agonists depending on the substitution pattern considered.^{31,32}

Thus, because little information has been published on structure–activity relationships (SAR) in the 6-aryl series of imidazobenzodiazepine esters, in this paper we report on the synthesis of the unusually substituted imidazo[1,5-*a*][1,4]benzodiazepine derivative **7** (along with its regioisomer **6**), which, acting as a partial agonist at CBR showed in some animal models a very interesting anxiolytic property in the absence of the unwanted effects typical of classic 1,4-benzodiazepines. Moreover, owing to the different behavior showed by compounds **6** and **7**, molecular modeling studies were performed with the double aim to define their binding modes within a model of GABA_A receptor and to account for their different intrinsic activity.

Chemistry

The synthesis of imidazoester **7** was carried out as depicted in Scheme 1.

Briefly, the synthetic strategy employed the noncommercially available 2-amino-5-fluoro-benzophenone **9** as the starting material. In fact, compound **9** was obtained by means of the sequential treatment of 5-fluoroanthranilic acid with phenyl lithium and chlorotrimethylsilane.³³ Regioselective nitration of

Scheme 1. Synthesis of Compound 7^a

^a Reagents and conditions: (i) $(\text{CH}_3)_3\text{SiCl}$, THF, 0 °C; (ii) KNO_3 , H_2SO_4 ; (iii) BrCH_2COBr , CH_2Cl_2 ; (iv) NH_3 , CH_3OH ; (v) $\text{ClPO}(\text{OEt})_2$, $t\text{-BuO}^-\text{K}^+$, dry THF; (vi) $\text{CNCH}_2\text{COOEt}$, $t\text{-BuO}^-\text{K}^+$.

benzophenone **9** in the presence of pure KNO_3 (99.9%) in concentrated H_2SO_4 afforded the hitherto unknown 2-amino-5-fluoro-3'-nitrobenzophenone **10**, which, by means of the sequential treatment with bromoacetyl bromide in dichloromethane and then with liquid ammonia in ethanol at reflux afforded 1,3-dihydro-7-fluoro-5-(3-nitrophenyl)-2H-1,4-benzodiazepin-2-one **11**. ^1H NMR spectrum of compound **10** along with ^1H NMR and X-ray diffraction studies performed on compound **11** (Figure 1), demonstrated the regioselectivity of the nitration at 3'-position, probably favored by the contemporary presence of the fluorine atom in the 5-position of benzophenone and the steric hindrance which prevents the reaction at 2'-position.

The imidazo-annulation of 1,4-benzodiazepin-2-one **11** accomplished via the intermediate enol phosphonate **12** by means

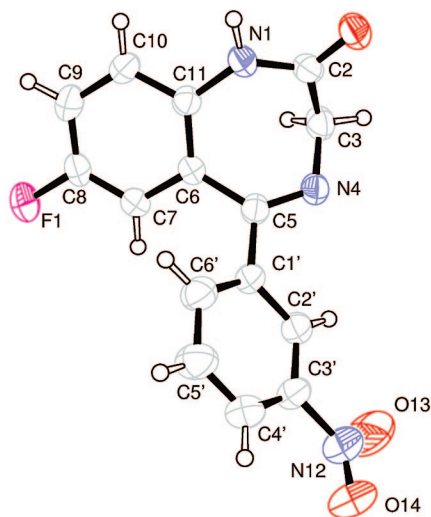
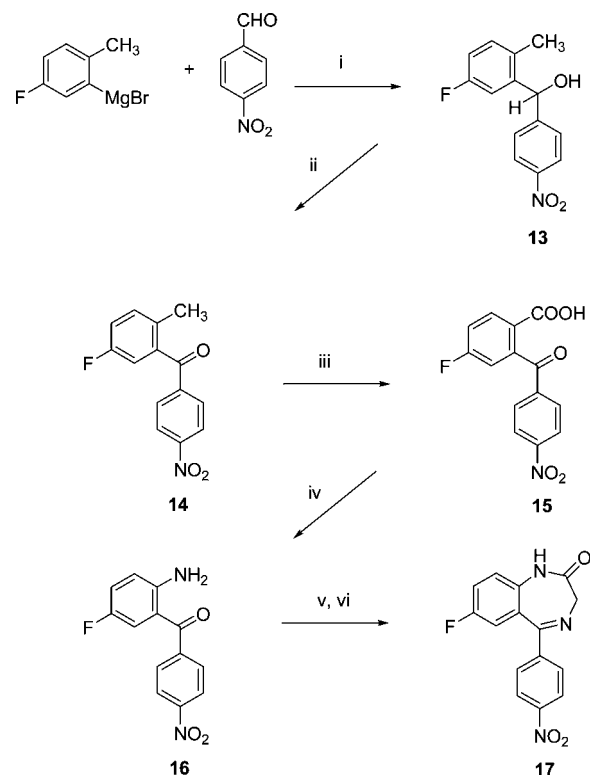


Figure 1. Crystal structure of compound **11** $\times \text{H}_2\text{O}$. Ellipsoids enclose 50% of probability. (The water molecule is omitted for the sake of clarity).

Scheme 2. Synthesis of Compound 17^a

^a Reagents and conditions: (i) toluene, -40 °C; (ii) $(n\text{-Bu})_4\text{N}^+\text{MnO}_4^-$, pyridine; (iii) KMnO_4 , pyridine/ H_2O ; (iv) DPPA, TEA, benzene; (v) BrCH_2COBr , CH_2Cl_2 ; (vi) NH_3 , CH_3OH , reflux.

of ethyl isocyanoacetate in the presence of potassium *tert*-butoxide, provided the imidazoester **7** in satisfactory yield.³⁴ The synthetic route used to prepare 2-amino-5-fluoro-4'-nitrobenzophenone **16** involved the low-temperature inverse addition of 4-fluoro-*o*-tolylmagnesium bromide to *p*-nitrobenzaldehyde to give 5-fluoro-2-methyl-4'-nitrobenzhydrol **13**.³⁵ Oxidation of this compound with tetrabutyl ammonium permanganate in pyridine gave 5-fluoro-2-methyl-4'-nitrobenzophenone **14**. Reoxidation of this compound in the presence of potassium permanganate afforded the benzoyl benzoic derivative **15**, which was converted in two steps into the aminobenzophenone **16** by reaction with diphenyl phosphorazidate (DPPA).³⁶ In this sequence, the resulting acyl azide underwent Curtius rearrangement to give the corresponding isocyanate derivative, which was promptly hydrolyzed into the expected 2-amino-5-fluoro-4'-nitrobenzophenone **16** (Scheme 2). The transformation of compound **16** into benzodiazepinone **17** and its successive imidazo-annulation following the above-reported procedure led to imidazoester **6**.

Results and Discussion

The binding affinity of the imidazo[1,5-*a*][1,4]benzodiazepine esters **6** and **7** at the benzodiazepine receptor in bovine and human cortical membranes was determined by means of competition experiments against the radiolabeled antagonist [^3H]flumazenil ([^3H]ethyl 8-fluoro-5,6-dihydro-5-methyl-6-oxo-4H-imidazo[1,5-*a*][1,4]benzodiazepine-3-carboxylate) and expressed as the K_i because these compounds inhibited radioligand binding by more than 80% at a fixed concentration of 10 μM . The *in vitro* efficacy of both compounds was measured by the GABA ratio, which predicts the pharmacological profile of a BzR ligand.^{16,37,38} The resultant value, expressed as a ratio of

Table 1. Inhibition of [^3H]Flumazenil Specific Binding to Bovine and Human Cortical Membranes and GABA Ratios of Imidazoesters **6** and **7**

compd	R	R ₁	K _i ^a (nM) bovine cortical membranes (SEM)	K _i ^a (nM) human cortical membranes (SEM)	GABA ratio ^b bovine cortical membranes	GABA ratio ^b human cortical membranes
5	H	4-NO ₂	1.80 (IC ₅₀) ^c		antagonist ^c	
6	F	4-NO ₂	14.80 ± 1.4	20.0 ± 1.8	0.89	0.86
7	F	3-NO ₂	4.40 ± 0.3	9.70 ± 0.7	1.19	1.20
flunitrazepam			5.17 ± 0.20	6.5 ± 0.5	1.68	1.60
flumazenil			1.90 ± 0.09	2.1 ± 0.08	1.03	1.01

^a K_i values are the means ± SEM of three independent determinations. ^b GABA ratio = (K_i without GABA/K_i with 50 μM GABA). ^c See ref 30.

K_i without GABA/K_i with GABA is nearly 2 for a full agonist, 1 for an antagonist; partial agonists are intermediate between 1 and 2, while a GABA ratio value below 1 is typical for inverse agonists. Table 1 summarizes the biological data, and it appears that both compounds **6** and **7** are able to bind to CBR with higher affinity for bovine cortical membranes than for the human ones, their K_i values being 14.80 and 4.40 nM vs 20.0 and 9.70 nM, respectively.

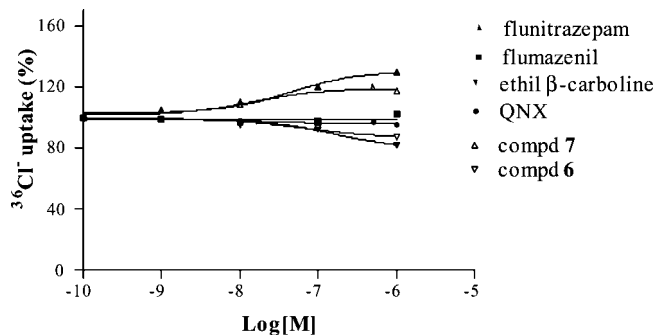
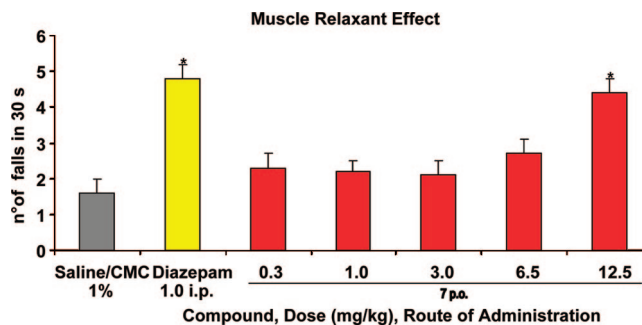
In particular, compound **7** appears as active as flunitrazepam, which shows a K_i of 5.15 nM but less potent than compound **5** (1.8 nM). These data suggest that the presence of a nitro substituent in the pendant phenyl ring of (iBDZ) leads to very active compounds, the affinity of which appears to be modified by the contemporary presence of the fluorine atom in position 8 of the iBz scaffold. The influence of 8-substitution is particularly evident in compound **6** and to a lesser extent in compound **7**, the affinity of which is moderately lower, being 2.5 and 8.2 times lower when compared to compound **5**, suggesting that the fluorine atom causes an ancillary interaction, which, though not detrimental, seems to be able to decrease to some extent the affinity of compounds **6** and **7** for CBR binding site. It is well-known that fluorine can induce significant stereoelectronic effects in the organic molecules in which it is inserted. The difference in electronegativity between carbon and fluorine generates a large dipole moment in this bond that, when combined with the electrostatic distribution of a specific molecule, may contribute to the molecule's ability to engage in intermolecular interactions.

This is particularly true in aromatic systems where the introduction of fluorine changes the electrostatic distribution of the molecular surface and may also induce new binding sites localized in the proximity of the fluorine atoms.³⁹

A second and more direct measure of in vitro efficacy was determined by a $^{36}\text{Cl}^-$ uptake assay measured in rat cerebrocortical synaptoneurosome.^{40,41} The synaptic chloride conductance effected by GABA activating the GABA_A receptor complex is modulated by ligands acting at the BzR. Full agonists increase the current, and antagonists have no effect, while inverse agonists decrease ion flow. The test compounds were compared to flunitrazepam, flumazenil, ethyl β-carboline, and to an imidazo[1,5-*a*]quinoxaline⁴² (which was resynthesized ad hoc and named QNX), being a full agonist, an antagonist, an inverse agonist, and a pure antagonist, respectively (Figure 2).

On the basis of the results obtained with these standards, it was possible to establish the course of the uptake and to make a direct comparison with the compounds analyzed. In particular, compounds **6** and **7** showed a partial decrease and a partial increase in the $^{36}\text{Cl}^-$ influx, respectively, confirming their efficacies as partial inverse agonist and partial agonist as was indicated by their respective GABA ratio value.

As for the different intrinsic activity at CBR elicited by compounds **6** and **7**, it is evident that 4'-nitro or 3'-nitro substitution is able to modulate the activity, leading to a partial inverse agonist [GABA ratio = 0.89 (bovine cortical membranes) or 0.86 (human cortical membranes)] or to a partial

**Figure 2.** $^{36}\text{Cl}^-$ uptake measured in rat cerebrocortical synaptoneurosome for Imidazoesters **6** and **7**.**Figure 3.** Effect on motor coordination 30 min after the treatment. Each value represents the mean of at least 15–20 mice $^{\wedge}P < 0.05$, $^*P < 0.01$ vs saline/CMC treated mice.

agonist [GABA ratio = 1.19 (bovine cortical membranes) or 1.20 (human cortical membranes)], respectively, suggesting that: (a) in accordance with what was previously stated, 4'-nitro substitution ensures no agonist activity to compound **6** but not necessarily leads to an antagonist;³⁰ (b) the hitherto unexplored 3'-nitro substitution, leading to a partial agonist endowed with a promising antianxiety activity, opens new sceneries in the study of central benzodiazepine receptor–ligand interactions.

Pharmacological Results

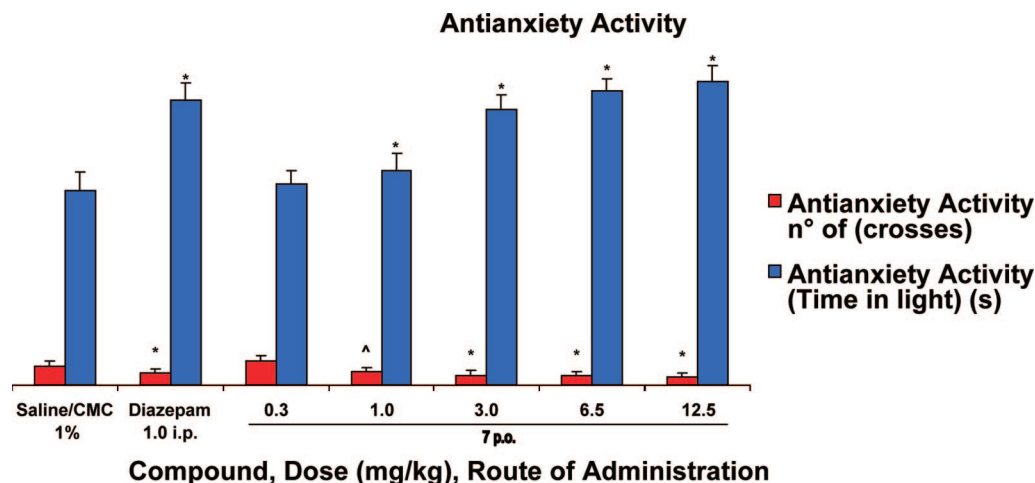
Compound **7** was examined in mice in vivo for its pharmacological effects. Five potential benzodiazepine actions were considered: the myorelaxant effect with the rota-rod, the anticonvulsant action evaluated by means of the new compound against pentilene-tetrazole-induced convulsions, potential anxiolytic effects screened using light/dark choice test; compound **7** was also tested for its ethanol-potentiating action, and finally the mouse learning and memory impairment was evaluated by passive avoidance test.

Effect on Motor Coordination. The effects of compound **7** on animal motor coordination was investigated using the mouse rota-rod test as the screening method to discover any myorelaxant effect (Figure 3). Compound **7** was tested in the range of doses between 0.3 and 12.5 mg kg⁻¹ po, and it statistically increased the number of falls showing a muscle relaxant effect

Table 2. Muscle Relaxant, Anticonvulsant, and Anxiolytic-Like Effects of Compound 7^a

treatment	mg/kg	muscle relaxant effect, rota-rod test		anticonvulsant activity against PTZ-induced attacks		antianxiety activity, light-dark box	
		no. of falls in 30 s		convulsion latency (min)	death latency (min)	no. of crosses	time (s) in light
		before treatment	30 min				
CMC 1% saline		5.0 ± 0.4	1.6 ± 0.0	18.0 ± 3.6	22.3 ± 4.4	11.4 ± 3.6	119.6 ± 11.5
diazepam	1.0 ip	4.8 ± 0.4	4.5 ± 0.4 ^c	no convulsion	no death	7.5 ± 2.1 ^c	175.3 ± 10.4 ^c
7	0.3po	4.6 ± 0.5	2.3 ± 0.4			14.6 ± 3.5	123.7 ± 8.5
7	1.0po	4.7 ± 0.4	2.2 ± 0.3			8.6 ± 2.2 ^b	132.0 ± 10.6 ^c
7	3.0po	5.1 ± 0.4	2.1 ± 0.4	18.7 ± 4.8	21.9 ± 5.3	5.6 ± 3.2 ^c	169.3 ± 9.6 ^c
7	6.5po	4.8 ± 0.3	2.7 ± 0.4	19.3 ± 4.5	22.5 ± 6.7	5.4 ± 3.1 ^c	181.2 ± 7.7 ^c
7	12.5po	4.7 ± 0.4	4.4 ± 0.4 ^c	23.6 ± 5.1	39.8 ± 7.1 ^c	5.1 ± 2.3 ^c	186.8 ± 9.9 ^c

^a Each value represents the mean of at least 15–20 mice. ^b $P < 0.05$. ^c $P < 0.01$ vs saline/CMC treated mice.

**Figure 4.** Effect on antianxiety activity. Each value represents the mean of at least 15–20 mice [^] $P < 0.05$, ^{*} $P < 0.01$ vs saline/CMC treated mice.

only at the highest dose employed; this effect is comparable to that exhibited by reference drug diazepam (1.0 mg kg⁻¹ ip).

Effect on Pentylentetrazole (PTZ)-Induced Convulsions. The anticonvulsant activity was studied by means of pentylentetrazole [6,7,8,9-tetrahydro-5H-tetrazoloazepine (PTZ)] as a chemical convulsant agent. Compound 7 at the same dose, which showed myorelaxant effect (12.5 mg kg⁻¹ po), was also able to increase the mouse death latency but not the convulsion latency. The anticonvulsant efficacy of compound 7 is lower than that of diazepam, which was able to completely prevent the attacks (Table 2). In the same experimental conditions, none of the other doses of compound 7 showed any anticonvulsant action.

Antianxiety Effect. Effects on mouse anxiety of newly synthesized molecule and diazepam were studied by a light/dark box apparatus. In our experiments, compound 7 showed a statistically significant anxiolytic-like effect starting from the dose of 1 mg kg⁻¹ po as demonstrated by both the reduction of transfer number from one compartment to the other and the increase of the time spent in the light compartment of the light/dark apparatus (Figure 4). Compound 7, at higher doses 3.0, 6.5, and 12.5 mg kg⁻¹ po, potentiated both parameters in a dose-dependent manner. Compound 7 showed an efficacy comparable to that of the reference drug, while the potency was lower than that of diazepam. The antianxiety action of compound 7 (3.0–12.5 mg kg⁻¹ po) was also confirmed in two other well-known tests used for the investigation of antianxiety-like effect: rat lick monitor suppression and rat elevated plus maze tests (data not shown).

Effect on Ethanol-Induced Sleeping Time. Compound 7, at the highest dose employed (12.5 mg kg⁻¹ po), potentiated the ethanol-endurance sleeping time without modifying the

induction time in statistically significant manner (Figure 5). The examined compound exerted an hypnotic effect at the same dose that exerted also myorelaxant and antianxiety action. Lower doses of compound 7 (3.0–6.5 mg kg⁻¹ po) were devoid of any activity on both induction and endurance time. As expected, diazepam at the dose of 1.0 mg kg⁻¹ ip exhibited hypnotic action as shown by the increase in ethanol-induced sleeping time.

Effects on Cognitive Processes. To investigate the effect that the new compound has on learning and memory, the mice performance on passive avoidance test was investigated. In this assay, the difference between the retention latencies of compound 7-treated mice and CMC-treated controls were statistically significant only at the highest dose (12.5 mg kg⁻¹ po) (Figure 6). Compound 7 showed an amnesic activity similar to that exerted by the reference drug diazepam (1.0 mg kg⁻¹ ip). Lower doses of compound 7 did not show any effect on learning and memory processes.

Molecular Modeling Studies. So far, several models of ligands interaction with ω modulatory sites have been reported in the literature.⁴⁶ These models subsequently started from the simple “two site hypothesis”,⁴⁷ made by one of us, according to which two sites are required for recognition at the ω modulatory sites: a condensed aromatic ring and an electron-donating group. The distance between these sites was assumed to modulate intrinsic activity (agonist and antagonist). An additional electron-donating site was included for antagonists and inverse agonists.³⁰ Progressing toward the Shove four-site model⁴⁸ surely contributed to a better understanding of ligand/receptor interaction. But all these models do not take into account the heterogeneity of the ω modulatory sites.

Cook and co-workers⁴⁹ very recently published an updated unified pharmacophore model for the benzodiazepine receptor

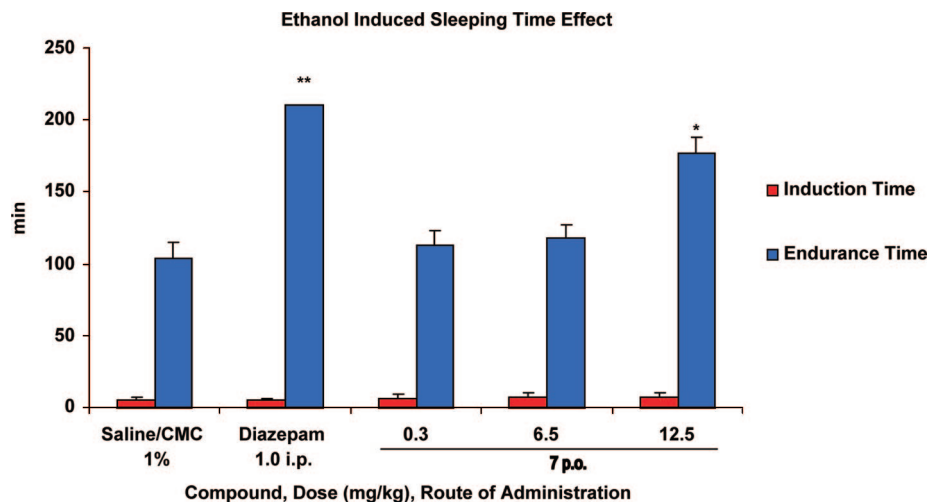


Figure 5. Sleeping time effect. Each value represents the mean of at least 15–20 mice $^{\wedge}P < 0.05$, $^*P < 0.01$ vs saline/CMC treated mice.

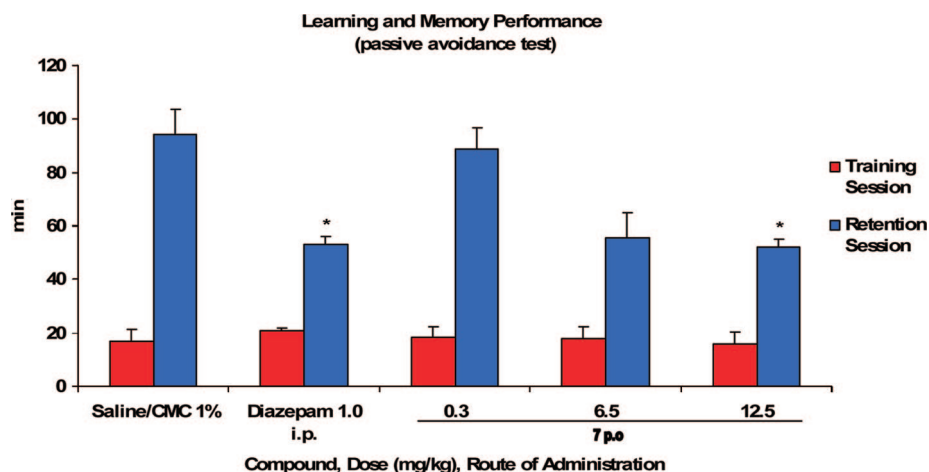


Figure 6. Learning and memory test. Each value represents the mean of at least 15–20 mice $^{\wedge}P < 0.05$, $^*P < 0.01$ vs saline/CMC treated mice.

based on structure–activity relationship studies of more than 150 different ligands from 15 structurally different classes of compounds. This model was developed by assuming that benzodiazepine receptor agonists, antagonists, and inverse agonists share the same binding pocket. It identifies receptor areas of special physicochemical properties that should be located in a well-defined spatial arrangement in order to be counterbalanced by the ligands. In the unified pharmacophore model, H_1 and A_2 are hydrogen bond donor and acceptor sites, respectively, whereas H_2/A_3 is a bifunctional hydrogen donor/acceptor site, L_1 , L_2 , L_3 , and L_{Di} are lipophilic pockets, and S_1 , S_2 and S_3 denote regions of negative steric interactions.

Through a deep examination of affinity and efficacy SAR, a ligand–receptor interaction was rationalized for the new imidazoesters **6** and **7**, assuming as topological model the above-cited pharmacophore/model proposed by Cook et al., which compounds **6** and **7** show to fit almost well. In particular, the imidazobenzodiazepine system binds the GABA/Bz complex through N_2 and N_5 atoms by means of a hydrogen bond involving H_1 and H_2 donor sites, respectively, and the lipophilic region L_1 appears to coincide with the benzofused moiety. However, the Cook's unified pharmacophore model seems not to be able to explain how the slight structural differences of compounds **6** and **7** are responsible for the opposite intrinsic activity (partial inverse agonist vs partial agonist) elicited, respectively, by the two compounds.

To better understand the ligand–receptor interactions, and with the aim to deepen their mode of binding, compounds **6** and **7** were submitted to molecular docking calculations by means of the homology model of the GABA_A receptor, proposed by Cromer et al. and built starting from the crystal structure of the *n*ACh receptor.⁵⁰ It is now well-established that the benzodiazepine binding site is located between α and γ subunits. Many residues involved in the benzodiazepine binding site have been identified through mutagenesis experiments and are shown in Figure 7.

It is also well-known that the benzodiazepine ring is not planar and it is able to adopt two preferred conformations that are in equilibrium, so it is difficult to assess unambiguously which of the two conformations is the bioactive one because many factors such as the presence of substituents on the diazepine ring as well as the receptor environment play a key role in determining the binding conformation.⁵¹

This is the reason why, in this study, both conformations were considered for compounds **6** and **7** having, respectively, the pendant phenyl ring flipping above and below the plane formed by the imidazofused moiety. For the sake of brevity, only the conformations of compound **7** are reported in Figure 8.

By means of the AutoDock program,⁵² the two conformations of compounds **6** and **7**, respectively, were subjected to 100 independent runs of docking simulations. Cluster analysis was then performed with a rms tolerance of 1.0 Å. The lowest energy

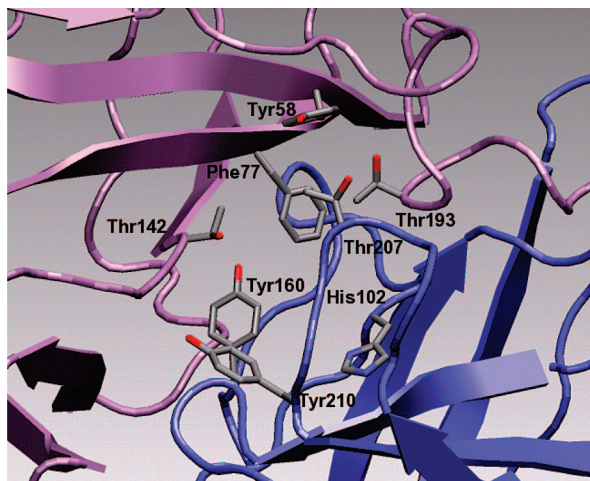


Figure 7. Representation of the structure of the benzodiazepine-binding site. The α - and γ -subunits are colored in blue and pink, respectively, while the main interacting residues are represented as atom type colored stick. Hydrogen atoms are not displayed for the sake of clarity.

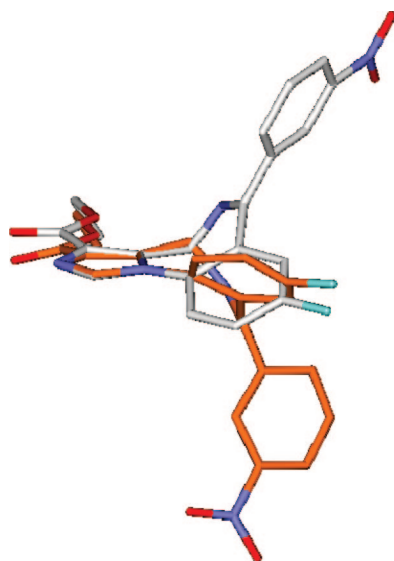


Figure 8. Two possible conformations of compound 7: (a) with the pendant phenyl ring above the imidazofused plane (white), (b) with the pendant phenyl ring below the imidazofused plane (orange).

solutions resulting from the four docking calculations in each case belong to the most populated cluster and were analyzed for their consistency with experimental data.

The results obtained from docking simulations of **6** and **7** suggest two alternative binding modes, one for each benzodiazepine ring conformation, here referred to as A and B. In the case of binding mode A, having the pendant phenyl ring above the imidazofused moiety, the estimated free energy of binding ($BE = -8.57$ kcal/mol for **6** and -10.86 kcal/mol for **7**) is in good accordance with the nanomolar experimental affinity data (Table 1). In a different way, binding mode B, which is individuated by the conformations having the pendant phenyl ring below the imidazofused moiety and endowed with an estimated free energy of binding, (-5.71 and -6.29 kcal/mol for **6** and **7**, respectively), correspond to a micromolar E_{K_i} in open contrast with the experimental binding data (Table 1).

In particular, the binding mode A of compounds **6** and **7** highlighted the aromatic interactions of the benzodiazepine moiety with hydrophobic residues such as Phe77, Phe100,

His102, Tyr160, Tyr210, and polar interactions established with Thr207 and Thr142 side chains.

On the other hand, in the alternative binding mode B, compounds **6** and **7** retain two polar interactions with Thr207 and Thr142, but three important aromatic interactions with Phe100, Tyr160, and Tyr210 are missing.

Thus, only the binding mode A is in full agreement with the experimental data according to which residues such as Tyr210, Phe77, and Thr207 are essential for benzodiazepines selectivity.⁵³ Furthermore, while it was demonstrated that Thr142 affects the efficacy of benzodiazepines,⁵⁴ His102 proved to be deeply involved in the benzodiazepines binding.⁵⁵ In addition, the replacement of Tyr160 by a serine residue resulted in the loss of [³H]flumazenil binding and it has also been suggested that Phe77 interacts with the pendant phenyl group of flumetazepam.⁵⁶

Consequently, taking into account the above-mentioned energetic differences and the agreement with the main mutagenesis data, the conformers with the pendant phenyl ring above the imidazofused moiety seem to represent the most probable receptor binding conformations (binding mode A) of both **6** and **7** (Figures 9 and 10).

According to our docking results, it clearly emerges that a network of aromatic interactions governs the binding of compounds **6** and **7**. Indeed, the pendant phenyl and the benzofused ring of the benzodiazepine moiety of both compounds were found to form an off-centered parallel displaced π - π interaction with Phe77 and His102, respectively, whereas the diazepine portion and the imidazofused ring forms stacking interactions with Tyr160 and Tyr210.

In particular, the benzofused ring was found to occupy a region shaped by His102, Asn103, and Phe100 in perfect agreement with a recent study highlighting the involvement of such residues in the imidazobenzodiazepines binding. Indeed, when His102, Asn103, and Phe100 were individually mutated into cysteine, they were found to interact covalently with 7-isothiocyano-1,4-benzodiazepines and the substituent at position 8 of the imidazobenzodiazepines like flumazenil, 8-azido-5,6-dihydro-5-methyl-6-oxo-4*H*-imidazo[1,5-*a*][1,4]benzodiazepine-3-carboxylic acid ethyl ester (Ro 15-4513), and imid-NCS compound.⁵⁷

As important as the hydrophobic interactions are the polar contacts between the carboxyethyl groups of both compounds and Thr207 and Thr142 side chains by means of two hydrogen bonds, while in the case of the partial agonist **7**, the 3'-nitro group is also able to form an additional hydrogen bond with Thr193 side chain (Figure 9).

It is worth noting that, in the case of the inverse agonist 4'-nitro derivative **6**, in all the binding conformations proposed by the docking program, no one showed a favorable interaction of the nitro group with any receptor counterpart (Figure 10).

Interestingly, the 5-nitro indole derivatives **8a** and **8c**, previously reported by Primofiore et al.,⁵⁸ are both endowed with a partial agonist activity ($GR = 1.17$ and $GR = 1.13$, respectively), while compounds **8d**, **8e**, and **8b** bearing a nitro group inserted in 4' position of the pendant phenyl ring, just as our compound **6**, show an inverse agonist activity (**8d**, $GR = 0.75$; **8e**, $GR = 0.73$; **8b**, $GR = 0.82$).⁵⁸ Intrigued by a possible role of the nitro group in the modulation of the intrinsic activity of ligands, we decided to dock all these derivatives into the Cromer's GABA_A receptor model. For all the indole derivatives, two main interactions were observed. The pendant phenyl ring of compounds **8a**, **8b**, **8d**, **8e**, and the indane fragment of **8c** were found to form an aromatic interaction with Tyr160, while

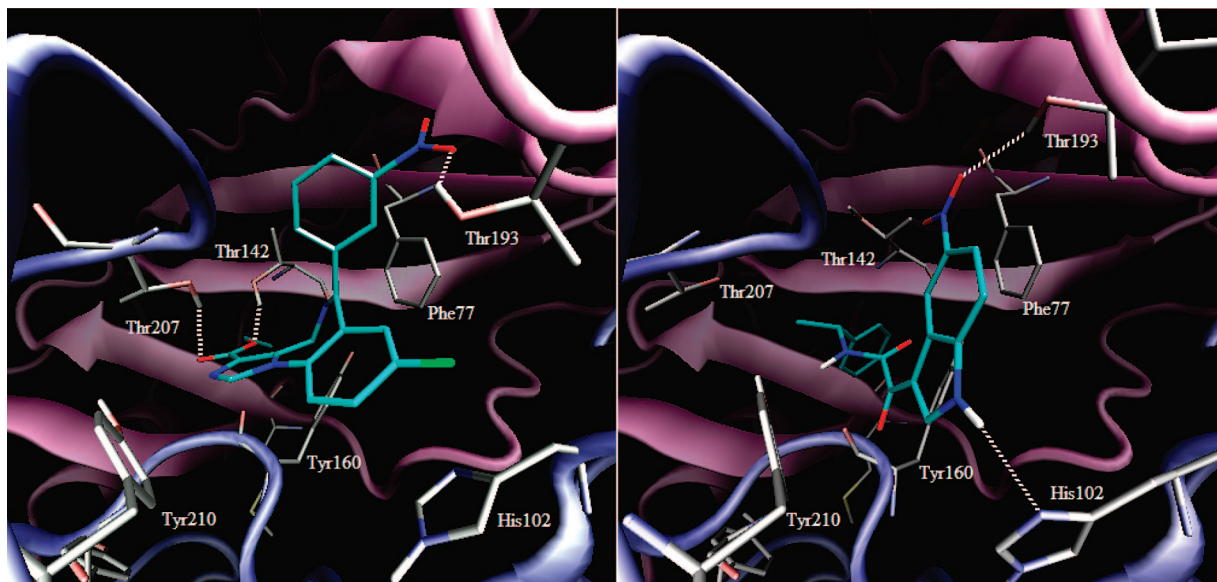


Figure 9. Compounds **7** and **8a** docked into the CBR binding site. The α - and γ -subunits are colored in blue and pink, respectively, while the main interacting residues are represented as atom type colored stick. Hydrogen bonds are indicated as white dashed lines.

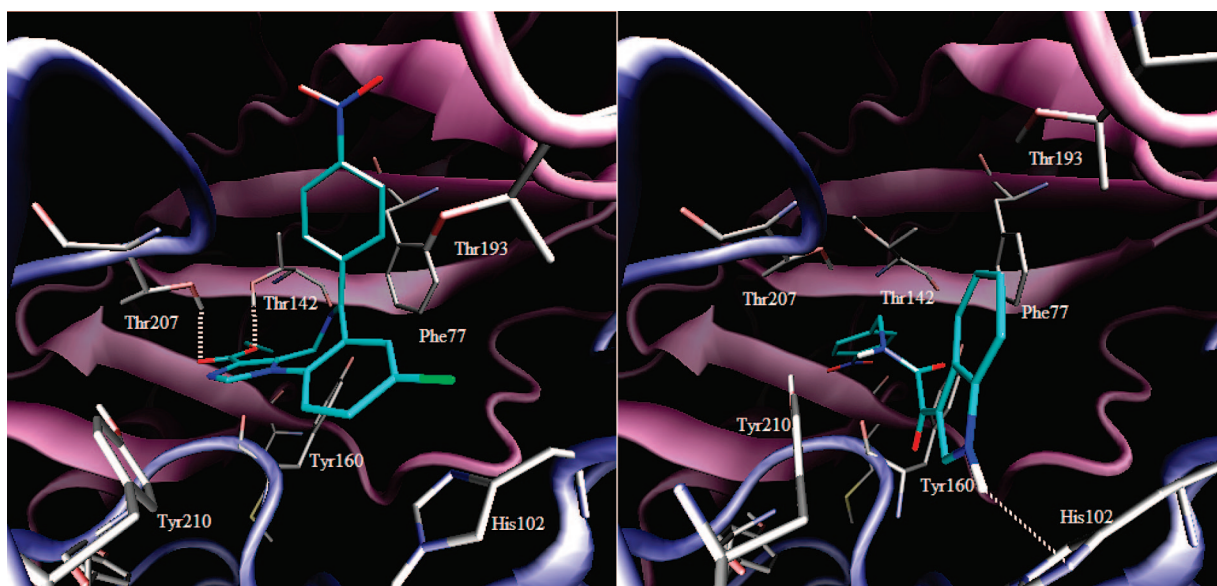


Figure 10. Compounds **6** and **8d** docked into the CBR binding site. The α - and γ -subunits are colored in blue and pink, respectively, while the main interacting residues are represented as atom type colored stick. Hydrogen bonds are indicated as white dashed lines.

a hydrogen bond between indole nitrogen and His102 occurred. Moreover, just for 5-nitro derivatives **8a** and **8c**, an aromatic interaction between the indole ring and the Phe77 was observed. For both compounds **8a** and **8c**, the 5-nitro group was found to form a hydrogen bond with Thr193, similarly to imidazobenzodiazepine **7** (Figure 9). On the contrary, in none of the inverse agonists **8d**, **8e**, and **8b**, the 4'-nitro group is capable of making such hydrogen bond being embedded in a pocket formed by residues Met130, Tyr141, Arg132, Ala161, and involved in a polar interaction with the Met130.

The binary complex formed by compound **7** and CBR was then subjected to an extensive molecular dynamics study (MD) (Figure 11) aiming at investigating the energy profile, the stability of the above-proposed binding mode, and the main intermolecular interactions based on a large time-scale simulation. During 3 ns of MD, the complex showed an energetic and geometric stable profile (see Supporting Information for more details), reinforcing the significance of our docking results.

Indeed, the binding mode of **7** does not substantially diverge from that calculated by AutoDock program, as it keeps all the above-described main interactions with the protein. In particular, the benzodiazepine moiety still engages stacking interactions with His102 and Tyr106 while the imidazofused ring improves the geometry of its π - π interaction with Tyr210 side chain. On the other hand, the phenyl pendant branch enforces its hydrophobic contacts by adding to the previously observed stacking with Phe77 a supplementary T-shaped interaction with Tyr58. Furthermore, during the whole MD simulation, the nitro group lies always near to Thr193 interacting with either the hydroxyl group or the backbone NH.

It is noteworthy that, during the production run, the polar interaction between the Thr142 side chain and the ester function of **7** was completely lost in favor of a new better directed H-bond of the Thr142 hydroxyl group with the N₅ of the diazepine ring. The ester function of **7**, on the contrary, makes a H-bond with one of the surrounding water molecules occupy-

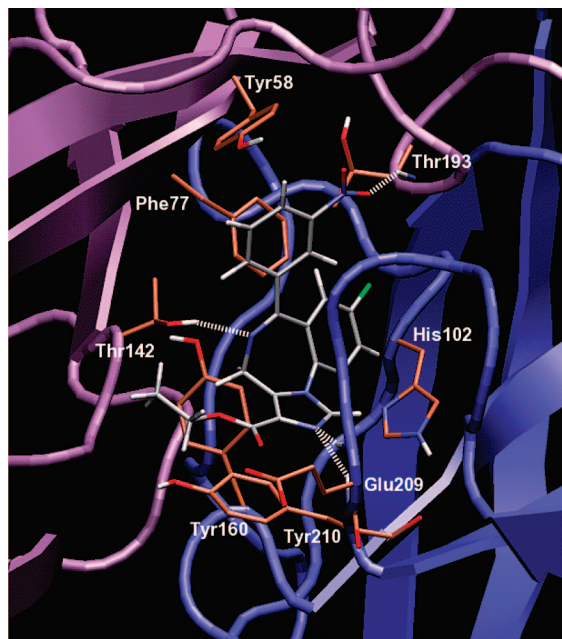


Figure 11. Snapshot of the MD simulation of the complex between compound **7** and CBR selected within a stable simulation interval. The main interacting residues and compound **7** are represented as stick colored by atom type. Proteins are represented as a cartoon with the α - and γ -subunits colored in blue and pink, respectively. For the sake of clarity, only polar hydrogens of the interacting residues are shown.

ing the region in apposition to Ala79, which was found to be involved in the binding of the substituent at position 3 of the imidazofused moiety by many experimental data.^{49,59}

The only striking difference between docking and MD results resides in the location of the imidazofused ring, which does not support any favorable interaction according to the docking results, while during MD simulation, it is permanently placed in such a way as to form a double H-bond with the backbone NHs of Glu209 and Tyr210.

Nevertheless, because several sources of variability such as the choice of the GABA_A receptor model with all its uncertainties (chosen template, correctness of the alignment, loops refinement) have been included in this study, the choice of the docking algorithm and the resulted binding modes of our compounds have to be interpreted at a qualitative level. As a general comment, the good coherency between the docking and the MD results supports our proposed binding mode of compound **7**, suggesting a pivotal role of the nitro group present in the pendant phenyl ring in determining the intrinsic activity of such imidazobenzodiazepine compounds.

Conclusion

Ethyl 8-fluoro-6-(3-nitrophenyl)- and ethyl 8-fluoro-6-(4-nitrophenyl)-4*H*-imidazo[1,5-*a*][1,4]benzodiazepine 3-carboxylate showed to be high affinity ligands for CBR. By control of NO₂ substituent at the 3'- and 4'-positions and halogen at the 8-position, analogues show a different efficacy from antagonist (**5**) and inverse agonist (**6**) to partial agonist (**7**). Most importantly, the 3'-nitrosubstituted imidazoester (**7**) with a partial agonist profile was identified and found active in selected animal models of anxiety.

So, consistently with the partial agonist hypothesis, side effects such as physical dependence, ethanol potentiation, and muscle relaxation were significantly reduced as compared to benzodiazepine full agonists. Compound **7** stands out as the one

having minimal benzodiazepine side effects yet is equieffective to diazepam in a classical animal model of anxiety such as the light–dark box test. Furthermore, SAR and different pharmacological profile of the title compounds were rationalized in terms of ligand interaction at CBR by means of a modeling study using the GABA_A receptor homology model developed by Cromer et al. According to docking and molecular dynamics simulations, it appears that the position of the nitro substituent in the ligands is considered responsible for the intrinsic activity although further experimental tests (e.g., synthesis of new ligands and receptor mutagenesis studies) are required to confirm such a hypothesis.

Experimental Section

Chemistry. All chemicals used were of reagent grade. Yields refer to purified products and are not optimized. Melting points were determined in open capillaries on a Gallenkamp apparatus and are uncorrected. Microanalyses were carried out by means of Perkin-Elmer 240C or a Perkin-Elmer series II CHNS/O analyzer, model 2400. Merck silica gel 60 (230–400 mesh) was used for column chromatography. Merck TLC plates and silica gel 60 F₂₅₄ were used for TLC. ¹H NMR spectra were recorded with a Bruker AC 200 spectrometer in the indicated solvent (TMS as internal standard). The values of the chemical shifts are expressed in ppm, and the coupling constants (*J*) are expressed in Hz. Mass spectra were recorded on a Varian Saturn 3 or a ThermoFinnigan LCQ-deca spectrometer.

Procedures for the Preparation of Substituted 2-Aminobenzophenones (9), (10), and (16). **2-Amino-5-fluorobenzophenone (9).** A stirred solution 1.25 M (titrated according to the literature procedure)⁶⁰ *n*-butyllithium in hexane (24.2 mL, 38.8 mmol) was treated dropwise at –40 °C with 2-bromobenzene (3.36 mL, 35.5 mmol) in dry diethyl ether (40 mL) over 0.5 h under a nitrogen atmosphere. The temperature was kept at –40 °C during the addition. The resulting dark-orange solution was stirred for a further 0.5 h at –40 °C. In a separate flask, a solution of 2-amino-5-fluorobenzoic acid (7.9 mmol) in dry THF (30 mL) also under a nitrogen atmosphere and at 0 °C (ice bath) was added in one portion to the solution prepared as described above, the mixture was stirred for 2 h at 0 °C and then treated with freshly distilled Me₃SiCl (20 mL, 160 mmol) steel under stirring. The reaction mixture was allowed to warm to room temperature (ca. 10 min.) and hydrolyzed with 1N HCl (60 mL). The resulting two-phase system was separated. The aqueous phase was neutralized with a 3N NaOH solution and extracted with diethyl ether (3 × 50 mL). The combined organic extractions were dried over Na₂SO₄, and the solvent was evaporated. The resulting brownish residue was purified by flash chromatography with dichloromethane as eluent. Recrystallization of the product from a methylene chloride/hexane mixture gave 2-amino-5-fluorobenzophenone as yellow needle-like crystals. Analytical and spectroscopic data were consistent with those reported in literature.⁶¹

2-Amino-5-fluoro-3'-nitrobenzophenone (10). A solution of potassium nitrate 99.9% (4.4 mmol) in 3.5 mL of concentrated sulfuric acid was added dropwise to a solution of 2-amino-5-fluorobenzophenone (**11**) in concentrated sulfuric acid (4.0 mL) kept at ice bath temperature. After addition was complete, the reaction mixture was stirred continuously in the ice bath for 30 min and then at room temperature for 4 h. The solution was poured into 100 mL of ice water and neutralized with concentrated ammonium hydroxide, giving a yellow precipitate that was collected by filtration and washed thoroughly with water until the washing was neutral. The precipitate was then dissolved into 150 mL of methylene chloride, and any insoluble material was removed by filtration. The filtrate was washed with water and brine, dried (magnesium sulfate), and filtered. The solvent was removed at reduced pressure, and the residue was recrystallized from methanol to give an analytical sample melting at 129–130 °C as pale-yellow needles.

5-Fluoro-2-methyl-4'-nitrobenzhydrol (13). To a suspension of magnesium turnings (7.2 mmol) in dry ether (10 mL), a solution

of 2-bromo-4-fluorotoluene (5.2 mmol) in dry ether (5.0 mL) was added dropwise. The mixture was refluxed for 30 min and, after cooling at room temperature, was cooled at -40°C . After the addition of a solution of 4-nitrobenzaldehyde (5.0 mmol) in dry toluene (35 mL) was completed, the mixture was stirred at -40°C for 1 h and then allowed to warm slowly to room temperature. 3N HCl (10 mL) was then added to decompose any remaining Grignard reagent. The organic phase layer was removed, washed with bicarbonate, and dried over magnesium sulfate. Evaporation of the solvent gave a brownish oily residue, which was purified by means of flash-chromatography, eluting with $\text{CHCl}_3/\text{EtOAc}$ (9:1 v/v) to give pure **13** as yellowish oil.

5-Fluoro-2-methyl-4'-nitrobenzophenone (14). To a solution of compound **13** (0.03 mmol) in dry pyridine (4.0 mL), tetrabutyl ammonium permanganate (0.08 mmol), dissolved in the same solvent (5.0 mL), was slowly added and the mixture, after keeping at room temperature for 20 min while stirring, was poured onto an ice-cooled solution of 2N HCl (20.0 mL) containing NaHSO_3 (0.8 mmol). The organic phase was removed and extracted with CHCl_3 , washed with water to neutrality, then with brine, and dried over sodium sulfate. After filtration and evaporation of the solvent the yellowish residue was flash-chromatographed using *n*-hexane/EtOAc 8:2 v/v as eluent to give pure **14** as a light-yellow solid. Recrystallization from methanol gave an analytical sample melting at $93\text{--}99^{\circ}\text{C}$ as colorless needles.

2-(4-Nitrobenzoyl)-4-fluorobenzoic Acid (15). To a solution of 5-fluoro-2-methyl-4'-nitrobenzophenone (**14**) (3.31 mmol) in pyridine (15 mL), H_2O (15 mL), and potassium permanganate (3.31 mmol) were added in sequence. The mixture was refluxed under stirring for 6 days, adding KMnO_4 (0.38 mmol) and a solution of H_2O /pyridine (1:1 v/v) (5.0 mL) every 24 h. When the reaction was completed, the mixture was cooled and MnO_2 formed was filtered off through celite. The acidification of the filtrate by means of 3N HCl gave a white precipitate, which was separated by filtration, washed to neutrality with water, and air-dried to give the expected acid fairly pure which was used as such in the next step.

2-Amino-5-fluoro-4'-nitrobenzophenone (16). To a mixture of compound **17** (0.34 mmol) in dry benzene (5.0 mL) in the presence of triethylamine (0.34 mmol), cooled at $0\text{--}5^{\circ}\text{C}$, DPPA (0.34 mmol) was added. The resulting mixture was stirred at room temperature for 3 h, heated to reflux for 4 h, and cooled, then 7 mL of 50% sulfuric acid were added. After overnight stirring at room temperature, the reaction mixture was poured into ice-water, made alkaline with concentrated NH_4OH and extracted with dichloromethane (3×20 mL). The combined extracts were washed to neutrality with water, dried over sodium sulfate, and concentrated under reduced pressure to give a residue as an orange solid. Purification of the residue by flash chromatography with dichloromethane as eluent gave pure **16** (0.19 mmol, 56%) as a yellow solid, which after recrystallization from methanol afforded an analytical sample melting at $146\text{--}147^{\circ}\text{C}$ as yellow prisms.

General Procedure for the Synthesis of Substituted 1,4-Benzodiazepinones (11) and (17). A solution of the suitable substituted 2-aminobenzophenone **10** or **16** (5.2 mmol) in dichloromethane (12 mL) was cooled in an ice bath. The mixture was stirred while a solution of bromoacetyl bromide (6.17 mmol) and an aqueous sodium carbonate solution (20%) were added alternatively, keeping the solution slightly basic. After the addition was completed, the reaction mixture was stirred at room temperature for 1 h. The precipitate formed was collected by filtration to afford the respective bromoacetanilide as an almost pure fine yellow powder which was used without any further purification in the next step. Approximately 100 mL of anhydrous liquid ammonia were condensed from a dry ice condenser in a stirred solution of the proper acetanilide (3.0 mmol) in dichloromethane (50 mL). After 4 h of reflux, the condenser was removed in order to allow the ammonia to evaporate. The solution was then washed with water until the washings were neutral, then washed with brine, dried over magnesium sulfate, and filtered. After the solvent was removed under reduced pressure, the correspondent 2-amino acetamide was obtained as a yellow oil. Without further purification, this compound

was heated to reflux in 50 mL of ethanol for 3 h in order to effect ring closure. On cooling, a yellow precipitate was formed and collected by filtration to give the expected substituted 1,4-benzodiazepinone **11** or **17**, which after recrystallization from the suitable solvent gave the corresponding analytical sample.

7-Fluoro-1,3-dihydro-5-(3-nitrophenyl)-2H-1,4-benzodiazepin-2-one (11). Pale-yellow needles from cyclohexane/EtOAc, mp $207\text{--}208^{\circ}\text{C}$ (yield 85%). ^1H NMR (CDCl_3) δ ppm: 4.35 (s, 2H), 6.92–6.97 (dd, 1H, $J = 2.23, 8.72$), 7.27–7.32 (m, 2H), 7.54–7.62 (t, 1H), 7.85–7.89 (t, 1H), 8.29–8.32 (d, 1H, $J = 6.55$), 8.42–8.44 (t, 1H), 9.85 (bs, 1H, exchangeable with D_2O).

7-Fluoro-1,3-dihydro-5-(4-nitrophenyl)-2H-1,4-benzodiazepin-2-one (17). Pale-yellow needles from cyclohexane/EtOAc, mp $211\text{--}212^{\circ}\text{C}$ (yield 78%). ^1H NMR (CDCl_3) δ ppm: 4.23 (s, 2H), 6.90–6.96 (dd, 1H, $J = 2.45\text{--}8.31$), 7.14–7.32 (m, 2H), 7.71–7.76 (d, 2H, $J = 8.76$), 8.22–8.26 (d, 2H, $J = 8.79$), 8.82 (bs, 1H, exchangeable with D_2O).

General Procedure for the Synthesis of Substituted 4H-Imidazo[1,5-a][1,4]benzodiazepine-3-ethoxycarbonyl Derivatives (6) and (7). A solution of the suitable 1,4-benzodiazepin-2-one (**11** or **17**) (1.21 mmol) and potassium *t*-butoxide (2.74 mmol) in dry THF (30 mL) was stirred in an ice bath for 10 min under nitrogen and was then treated with diethyl chlorophosphate (4.63 mmol). After stirring for 30 min, ethyl isocynoacetate (6.1 mmol) and potassium *t*-butoxide (6.6 mmol) were added (the solution turned dark brown). The mixture was continuously stirred in the ice bath for 1 h, was allowed to stir at room temperature overnight under nitrogen and after addition of acetic acid (1.8 mL), was stirred for an additional 20 min, and was then poured onto crushed ice to give a brownish solid. After filtration, the solid was dissolved into dichloromethane and the organic layer washed with brine, dried over Na_2SO_4 , filtered, and concentrated in vacuo. The residue purified by flash-chromatography eluting with the suitable solvent afforded the expected imidazoester **6** or **7** as a yellow solid, which after a recrystallization from the suitable solvent gave an analytical sample.

Ethyl 8-fluoro-6-(4-nitrophenyl)-4H-imidazo[1,5-a][1,4]benzodiazepine-3-carboxylate (6). Pale-yellow needles from benzene/cyclohexane mp $217\text{--}218^{\circ}\text{C}$ (yield 30%). ^1H NMR (CDCl_3) δ ppm: 1.38–1.45 (t, 3H, $J = 7.08$), 4.13 (bs, 1H), 4.40–4.43 (q, 2H, $J = 7$), 6.12 (bs, 1H), 7.03–7.09 (dd, 1H, $J = 2.62, 8.12$), 7.38–7.48 (m, 1H), 7.60–7.67 (m, 1H), 7.69–7.73 (d, 2H, $J = 8.72$), 7.91 (s, 1H), 8.21–8.25 (d, 2H, $J = 8.65$). MS: m/z 394 ($\text{M}^+ 70$).

Ethyl 8-Fluoro-6-(3-nitrophenyl)-4H-imidazo[1,5-a][1,4]benzodiazepine-3-carboxylate (7). Pale-yellow platelets from EtOAc/MeOH, mp $222\text{--}223^{\circ}\text{C}$ (yield 30%). ^1H NMR (CDCl_3) δ ppm: 1.38–1.45 (t, 3H, $J = 7.38$), 4.09 (bs, 1H), 4.36–4.47 (q, 2H, $J = 7.08$), 6.11 (bs, 1H), 7.06–7.12 (dd, 1H, $J = 2.8, 8.63$), 7.39–7.49 (m, 1H), 7.53–7.68 (m, 2H), 7.89–7.93 (d, 2H, $J = 7.89$), 8.23–8.28 (d, 1H, $J = 7.99$), 8.36 (s, 1H). MS: m/z 394 ($\text{M}^+ 70$).

X-Ray Crystallography. A single crystal of **11** $\times \text{H}_2\text{O}$ was submitted to X-ray data collection by means of a Siemens P4 four-circle diffractometer at 293 K equipped with a graphite monochromated Mo K α radiation ($\lambda = 0.71069 \text{ \AA}$). The structure was solved by direct methods implemented in the SHELXS-97 program.⁶² The refinements were carried out by full-matrix anisotropic least-squares on F^2 for all reflections for non-H atoms by means of the SHELXL-97 program.⁶³

Crystallographic data (excluding structure factors) of this crystal structure have been deposited with the Cambridge Crystallographic Data Centre as supplementary publication numbers CCDC 675538 (**11** $\times \text{H}_2\text{O}$). Copies of the data can be obtained, free of charge, on application to CCDC, 12 Union Road, Cambridge CB2 1EZ, UK [fax: 144-(0)1223-336033 or E-mail: deposit@ccdc.cam.ac.uk].

Radioligand Binding Studies. [^3H]flumazenil (specific activity 70.8 Ci/mmol) was obtained from Perkin-Elmer Life Science (Milan, Italy). All other chemicals were reagent grade and were obtained from commercial suppliers.

Bovine cortex was obtained from the local slaughterhouse. Human cortex samples were taken postmortem at the Department

of Pathological Anatomy, University of Pisa, during autopsy sessions. The subjects had died from causes not primarily involving the brain and had not suffered from any psychiatric or neurological disorders. The time between death and tissue dissection/freezing ranged from 18 to 36 h. The samples were immediately packed in dry ice and stored in a -80° freezer. The study was approved by the Ethics Committee of the University of Pisa, Italy.

Bovine and human cerebral cortex membranes were prepared in accordance with Martini et al.⁶⁴ Briefly, cerebral cortex were homogenized in 10 volumes of ice cold 0.32 M sucrose containing protease inhibitors. The homogenate was centrifuged at 1000g for 10 min at 4°C . the resulting pellet was discarded and the supernatant was recentrifuged at 48000g for 15 min at 4°C . Then the pellet was osmotically shocked by suspension in 10 volumes of 50 mM Tris-citrate buffer at pH 7.4 containing protease inhibitors and recentrifuged at 48000g for 15 min at 4°C . The resulting membranes were frozen and washed by means of a procedure previously described for removing endogenous GABA from cerebral cortex.⁶⁵ Finally, the pellet was suspended in 10 volumes of 50 mM Tris-citrate buffer pH 7.4 and used in the binding assay. Protein concentration was assayed by the method of Lowry et al.⁶⁶ using bovine serum albumin as the standard. [^3H]flumazenil binding studies were performed as previously reported.⁶⁷ The [^3H]flumazenil binding was performed in triplicate by incubating aliquots of the membrane fractions (0.2–0.3 mg of protein) at 0°C for 90 min in 0.5 mL of 50 mM Tris-citrate buffer, pH 7.4, with approximately 0.2 nM [^3H]flumazenil. Nonspecific binding was defined in the presence of 10 μM diazepam. After incubation, the samples were diluted at 0°C with 5 mL of the assay buffer and immediately harvested onto GF/B filters (Brandel) by means of a harvester and washing with ice-cold assay buffer. The filters were washed twice with 5 mL of the buffer, dried, and 4 mL of Ready Protein Beckman scintillation cocktail added; radioactivity was counted in an Packard LS 1600 liquid-phase scintillation β counter.

Compounds were routinely dissolved into DMSO and added to the assay mixture to make a final volume of 0.5 mL. Blank experiments were carried out to determine the effect of the solvent (2%) on binding. At least six different concentrations spanning 3 orders of magnitude, adjusted approximately for the IC_{50} of each compound, were used. IC_{50} values, computer-generated by a nonlinear formula on a computer program (GraphPad, San Diego, CA), were converted to K_i values, knowing the K_d values of radioligand in these different tissues calculated by the Cheng and Prusoff equation.⁶⁸ The K_d of [^3H]flumazenil binding to cortex membrane from bovine and human was 0.85 and 0.91 nM, respectively. The GABA ratio was determined by calculating K_i without GABA/ K_i with GABA 50 μM for each compounds.

Functional Efficacy Studies. ($^{36}\text{Cl}^-$ Uptake Studies). $^{36}\text{Cl}^-$ (specific activity 9.69 $\mu\text{Ci/g}$) was obtained from Perkin-Elmer Life Science (Milan, Italy). All other chemicals were reagent grade and were obtained from commercial suppliers.

$^{36}\text{Cl}^-$ uptake was measured in rat cerebrocortical synaptoneurosome as described by Schwartz et al.⁶⁹ with minor modifications. Briefly, cerebral cortex was dissected from Sprague–Dawley male rats suspended 1:10 with ice-cold solution containing 145 mM NaCl, 5 mM KCl, 5 mM MgCl_2 , 1 mM CaCl_2 , 10 mM HEPES, pH 7 (T1 buffer), and 10 mM D-glucose; they were homogenized with a glass–glass homogenizer (five strokes) and filtered through three layers of nylon mesh (160 μm) and a 10 μm Millipore filter. The filtrates were centrifuged at 1000g for 15 min. After discarding the supernatant, the pellet was gently resuspended in T1 buffer and washed once more by centrifugation (1000g for 15 min). The final pellet containing the synaptoneurosome was suspended 1:2 in T1 buffer was kept on ice until ready for assay (no longer than 30 min).

Aliquots of synaptoneurosome suspensions (1.5–2 mg of protein) were preincubated at 30°C for 10 min prior to the addition of 0.2 μCi of $^{36}\text{Cl}^-$. Drugs were added simultaneously with the $^{36}\text{Cl}^-$ (0.35 mL total assay volume). $^{36}\text{Cl}^-$ uptake was stopped 10 s later by the addition of 5 mL of ice-cold HEPES, followed by vacuum filtration through glass fiber filters (Whatman GF/B) that had been

soaked with 0.05% polyethylenimine to reduce nonspecific binding of $^{36}\text{Cl}^-$. The filters were washed three more times with 5 mL of ice-cold buffer and placed into scintillation vials containing 4 mL of Ready Protein Beckman scintillation cocktail and radioactivity was counted in a Packard LS 1600 liquid-phase scintillation β counter.

Data are expressed as percent stimulation of $^{36}\text{Cl}^-$ uptake above basal level.

Pharmacological Methods. The experiments were carried out in accordance with the Animal Protection Law of the Republic of Italy, DL no. 116/1992, based on the European Communities Council Directive of 24 November 1986 (86/609/EEC). All efforts were made to minimize animal suffering and to reduce the number of animals involved. Male CD-1 albino mice (22–24 g) and male Swiss Webster (20–26 g) (Morini Italy) were used. Twelve mice were housed per cage and fed a standard laboratory diet, with tap water ad libitum for 12 h/12 h light/dark cycles (lights on at 7:00). The cages were brought into the experimental room the day before the experiment, for acclimatization purposes. All experiments were performed between 10:00 and 15:00.

Rota-Rod Test. The integrity of the animals' motor coordination was assessed using a rota-rod apparatus (Ugo Basile, Varese, Italy) at a rotating speed of 16 rpm. The treatment was performed before the test. The numbers of falls from the rod were counted for 30 s, 30 min after drug administration, and the test was performed according to the method described by Vaught et al.⁷⁰

Light/Dark Box Test. The apparatus (50 cm long, 20 cm wide, and 20 cm high) consisted of two equal acrylic compartments, one dark and one light, illuminated by a 60 W bulb lamp and separated by a divider with a 10 cm \times 3 cm opening at floor level. Each mouse was tested by placing it in the center of the lighted area, away from the dark one, and allowing it to explore the novel environment for 5 min. The number of transfers from one compartment to the other and the time spent in the illuminated side were measured. This test exploited the conflict between the animal's tendency to explore a new environment and its fear of bright light.⁷¹

Pentylenetetrazole (PTZ)-Induced Seizure. PTZ (90 mg/kg sc) was injected 30 min after the administration of drugs. The frequency of the occurrence of clonic generalized convulsions was noted over a period of 30 min.⁷²

Passive-Avoidance Test. The test was performed according to the step-through method described by Jarvik et al.⁷³ The apparatus consisted of a two-compartment acrylic box with a lighted compartment connected to a darkened one by a guillotine door. As soon as the mouse entered the dark compartment, it received a thermal shock punishment. The latency times for entering the dark compartment were measured in the training test and after 24 h in the retention test. The maximum entry latency allowed in the training and retention sessions was, respectively, 60 and 180 s.

Ethanol-Induced Sleeping Time Test. Ethanol (4 g/kg ip) was injected 30 min after drug administration. The duration of a loss of the righting reflex was measured as the sleep time. The endpoint was recorded as 210 min.

Drugs. Diazepam (Valium 10) (Roche) and Pentylenetetrazole (PTZ) (Sigma) were used. All drugs were dissolved into isotonic (NaCl 0.9%) saline solution and injected sc/ip. The new compound was administered by the po route and was suspended in 1% carboxymethylcellulose sodium salt and sonicated immediately before use. Drug concentrations were prepared in such a way that the necessary dose could be administered in a 10 mL/kg volume of carboxymethylcellulose (CMC) 1% by the po, ip, or sc routes.

Statistical Analysis. All experimental result are given as the mean \pm SEM. An analysis of variance, ANOVA, followed by Fisher's protected least significant difference procedure for post hoc comparison, were used to verify significance between two means of behavioral results. The data were analyzed with the StataView software for Macintosh (1992). *P* values of less than 0.05 were considered significant.

Docking Calculations. All the ligands were docked into the CBR model by means of AUTODOCK 3.0 program.

Docking simulations of the compounds were carried out by means of the Lamarckian Genetic Algorithm⁵² and applying a protocol with an initial population of 50 randomly placed individuals, a maximum number of 1.0×10^6 energy evaluations, a mutation rate of 0.02, a crossover rate of 0.80, and an elitism value of 1. The pseudo-Solis and Wets algorithm with a maximum of 300 interactions was applied for the local search. One hundred independent docking runs were carried out for each ligand, and the resulting conformations that differ by less than 1.0 Å in positional root-mean-square deviation (rmsd) were clustered together. The conformer with the lowest free energy of binding was taken as the representative of each cluster.

Ligand Setup. The structures of the ligands were generated by means of Discovery Studio software version 1.5. Minimizations energies were achieved by means of the CHARMM force field⁷⁴ as implemented in Discovery Studio. Minimizations were carried out by means of 50 steps of steepest descent and 10000 steps of conjugate gradient as minimization algorithms, with a rms convergence criterion of 0.01 Å. Partial atomic charges were assigned by means of the Gasteiger–Marsili formalism.⁷⁵ All the relevant torsion angles were treated as rotatable during the docking process, allowing thus a search of the conformational space.

Protein Setup. The GABA_A receptor model was set up for docking as follows: polar hydrogens were added by means of Discovery Studio software version 1.5, Kollman united-atom partial charges were assigned. ADDSOL utility of the AutoDock program was used to add salvation parameters to the protein structures, and the grid maps representing the proteins in the docking process were calculated by means of AutoGrid. The grids, one for each atom type in the ligand, plus one for electrostatic interactions, were chosen to be large enough to include not only the hypothetical benzodiazepine binding site but also a significant part of the protein around it. As a consequence, for all docking calculations, the dimensions of grid map was 46 Å × 50 Å × 56 Å with a grid-point spacing of 0.375 Å.

Energy Refinement of the CBR/Ligand Complexes. The complexes obtained were subjected to an energy minimization by means of CHARMM force field as implemented in Discovery Studio. Energy optimizations were carried out by means of 200 steps of steepest descent followed by 10000 steps of conjugated gradient with an rms of 0.01 as gradient value.

Molecular Dynamics Simulations. The pose representative of the most populated cluster for compound **7** was used as the starting point for further molecular dynamics simulations.

The binary complex between the benzodiazepine receptor and (**7**) was subjected to a molecular dynamics study (MD) by means of NAMD2 molecular dynamics simulation code.⁷⁶ Three ns MD simulations on the complex were carried out in explicit solvent and periodic boundary conditions. Protein and ligand were parametrized by using Xleap module of AMBER⁷⁷ and the parm99 version⁷⁸ of the all-atom Amber force field.⁷⁹ The complex was subjected to the following procedure prior to molecular dynamics data collection: the complex was surrounded by a box of 6 Å layer of TIP3P31 pre-equilibrated water molecules⁸⁰ and neutralized by randomly placing 2 Cl[−] ions by means of the solvate and add ions routine of Xleap, respectively. A two-step preliminary minimization was carried out by means of a sophisticated conjugate gradient and line search algorithm, minimizing in the first 2000 steps water, counterions, and hydrogens, and in the following 2000 steps, the loops and all the side chains of the protein. A convergence criterion on the gradient of 0.0001 kcal mol^{−1} Å^{−1} was established. The microcanonical NVE ensemble (constant volume and energy) was used to raise the system temperature to 300 K during 43 ps of Langevin dynamics simulations with starting 5 kcal/mol Å² restraints on protein backbone atoms and on the ligand heavy atoms, which were gradually decreased during the heating. The system was then equilibrated with respect to volume running for 70 ps in NPT conditions (constant pressure and temperature) until all the restraints were left off. Langevin dynamics was used to keep the temperature constant (300 K) while the pressure (1 atm) was controlled

by means of the Langevin piston Nose–Hoover method.⁸¹ Eventually 3 ns of production run in NPT ensemble were carried out.

Van der Waals and short-range electrostatic interactions were estimated within a 10 Å cutoff with the switch value set at 8 Å and the pair list distance extended to 13.5 Å. The long-range electrostatic interactions were assessed by using the particle mesh Ewald (PME) method,⁸² with a grid size set to 100, 80, and 90 for *x*, *y*, and *z* axes, respectively, interpolated with a fourth-order function and by setting the direct sum tolerance to 10^{−5}.

All the simulations of the solvated complex were performed with a time step of 2 fs in combination with the SHAKE⁸³ algorithm to constrain bond lengths involving hydrogen atoms. Trajectory coordinates were saved every 2500 steps.

All calculations were performed on a Linux dual-core machine.

The VMD program was used for visualization and data analysis.⁸⁴

Acknowledgment. We are grateful to Dr Laura Salvini (C.I.A.D.S., University of Siena, Italy) for the recording of the mass spectra, to Prof. Stefania D'Agata D'Ottavi for the careful reading of the manuscript, and Consorzio Interuniversitario Nazionale per la Scienza e la Tecnologia dei Materiali (INSTM) for the access to Accelrys software. We are also grateful to Prof. Cromer for kindly providing us with the homology model of the GABA_A receptor. This work was financially supported by Consiglio Nazionale delle Ricerche (CNR) and Ministero dell'Università e della Ricerca (MIUR)—Programmi di Ricerca di Rilevante Interesse Nazionale (PRIN).

Supporting Information Available: Analytical data of compounds **6** and **7**, pharmacological data, docking, and molecular dynamics calculations. This material is available free of charge via the Internet at <http://pubs.acs.org>.

References

- (1) Kaupmann, K.; Huggel, K.; Heid, J.; Flor, P. J.; Bischoff, S.; Mickel, S. J.; McMaster, G.; Angst, C.; Bittiger, H.; Froestl, W.; Bettler, B. Expression Cloning of GABA-B Receptors Uncovers Similarity to Metabotropic Glutamate Receptors. *Nature* **1997**, *386*, 239–246.
- (2) Rabow, L. E.; Russek, S.H.; Farb, D. H. From Ion Currents to Genomic Analysis: Recent Advances in GABA_A Receptor Research. *Synapse* **1995**, *21*, 189–274.
- (3) Johnston, G.A.R. GABA_C Receptors: Relatively Simple Transmitter-Gated Ion Channels. *Trends Pharmacol. Sci.* **1996**, *17*, 319–323.
- (4) Skolnick, P.; Paul, S. The Benzodiazepine/GABA Receptor Chloride Channel Complex. *ISI Atlas Pharmacol.* **1988**, *2*, 19–22.
- (5) Doble, A.; Martin, I. L. Multiple Benzodiazepine Receptors: No Reason for Anxiety. *Trends Pharmacol. Sci.* **1992**, *13*, 76–81.
- (6) Nayeem, N.; Green, T. P.; Martin, J. L.; Barnard, E. A. Quaternary Structure of the Native GABA_A Receptor Determined by Electron Microscopic Image Analysis. *J. Neurochem.* **1994**, *62*, 815–818.
- (7) Rudolph, U.; Crestani, F.; Möhler, H. GABA_A Receptor Subtypes. Dissecting their Pharmacological Functions. *Trends Pharmacol. Sci.* **1999**, *22*, 188–194.
- (8) Sieghart, W.; Sperk, G. Subunit Composition, Distribution and Function of GABA-A Receptor Subtypes. *Curr. Top. Med. Chem.* **2002**, *2*, 795–816.
- (9) Ernst, M.; Brauchart, D.; Boresch, S.; Sieghart, W. Comparative Modeling of GABA-A Receptor: Limits, Insights, Future Developments. *Neuroscience* **2003**, *119*, 933–943.
- (10) Barnard, E. A.; Skolnick, P.; Olsen, R. W.; Möhler, H.; Sieghart, W.; Biggio, G.; Braestrup, C.; Bateson, A. N.; Langer, S. Z. International Union of Pharmacology. XV. Subtypes of γ -Aminobutyric Acid_A Receptors: Classification on the Basis of Subunit Structure and Receptor Function. *Pharmacol. Rev.* **1998**, *50*, 291–313.
- (11) Pritchett, D. B.; Luddens, H.; Seeburg, P. H. Type I and type II GABA_A-Benzodiazepine Receptors Produced in Transfected Cells. *Science* **1989**, *245*, 1389–1392.
- (12) Luddens, H.; Pritchett, D. B.; Kohler, M.; Killisch, I.; Keinänen, L.; Monyer, H.; Sprengel, R.; Seeburg, P. H. Cerebellar GABA_A-Receptor Selective for a Behavioural Alcohol Antagonist. *Nature* **1990**, *346*, 648–651.
- (13) Möhler, H.; Crestani, F.; Rudolph, U. GABA_A-Receptor Subtypes: A New Pharmacology. *Curr. Opin. Pharmacol.* **2001**, *1*, 22–25.
- (14) Whiting, P. J. Receptor Subtypes in the Brain: a Paradigm for CNS Drug Discovery. *Drug Discovery Today* **2003**, *8*, 445–450.

- (15) Collins, I.; Moyes, C.; Davey, W. B.; Rowley, M.; Bromidge, F. A.; Quirk, K.; Atack, J. R.; McKernan, R. M.; Thompson, S. A.; Wafford, K.; Dawson, G. R.; Pike, A.; Sohal, B.; Tsou, N. N.; Ball, R. G.; Castro, J. L. 3-Heteroaryl-2-pyridones: Benzodiazepine Site Ligands with Functional Selectivity for R2/R3-Subtypes of Human GABAA Receptor-Ion Channels. *J. Med. Chem.* **2002**, *45*, 1887–1900.
- (16) Braestrup, C.; Nielsen, M.; Honoré, T.; Jensen, L. H.; Petersen, E. N. Benzodiazepine Receptor Ligands with Positive and Negative Efficacy. *Neuropharmacology* **1983**, *22*, 1451–1457.
- (17) Haefely, W.; Kyburz, E.; Gerecke, M.; Möhler, H. Recent Advances in the Molecular Pharmacology of Benzodiazepine Receptors and in the Structure–Activity Relationships of their Agonists and Antagonists. *Adv. Drug Res.* **1985**, *14*, 165–322.
- (18) Julou, L.; Blanchard, J. C.; Dreyfus, J. F. Pharmacological and Clinical Studies of Cyclopyrrolones: Zopiclone and Suriclone. *Pharmacol., Biochem. Behav.* **1985**, *23*, 653–659.
- (19) Arbilla, S.; Depoortere, H.; George, P.; Langer, S. Z. Pharmacological Profile of the Imidazopyridine Zolpidem at Benzodiazepine Receptors and Electrocorticogram in Rats. *Naunyn–Schmiedeberg's Arch. Pharmacol.* **1985**, *330*, 248–251.
- (20) Malatynska, E.; Serra, M.; Ikeda, M.; Biggio, G.; Yamamura, H. Modulation of GABA-Stimulated Chloride Influx by β -Carbolines in Rat Brain Membrane Vesicles. *I. Brain Res.* **1988**, *443*, 395–397.
- (21) Gardner, C. R.; Tully, W. R.; Hedgecock, C. J. R. The Rapidly Expanding Range of Neuronal Benzodiazepine Receptor Ligands. *Prog. Neurobiol.* **1993**, *40*, 1–61.
- (22) Kahnberg, P.; Lager, E.; Rosenberg, C.; Schougaard, J.; Camet, L.; Sterner, O.; Østergaard Nielsen, E.; Nielsen, M.; Liljefors, T. Refinement and Evaluation of a Pharmacophore Model for Flavone Derivatives Binding to the Benzodiazepine Site of the GABA_A Receptor. *J. Med. Chem.* **2002**, *45*, 4188–4201.
- (23) Lager, E.; Andersson, P.; Nilsson, J.; Pettersson, I.; Østergaard Nielsen, E.; Nielsen, M.; Sterner, O.; Liljefors, T. 4-Quinolone Derivatives: High-Affinity Ligands at the Benzodiazepine Site of Brain GABA_A Receptors. Synthesis, Pharmacology, and Pharmacophore Modelling. *J. Med. Chem.* **2006**, *49*, 2526–2533.
- (24) Jensen, M. S.; Lambert, J. D. C. The Interaction of the beta-Carboline Derivative DMCM with Inhibitory Amino Acid Responses on Cultured Mouse Neurons. *Neurosci. Lett.* **1983**, *40*, 175–179.
- (25) Gardner, C. R. Pharmacological Profiles in vivo of Benzodiazepine Receptor Ligands. *Drug Dev. Res.* **1988**, *12*, 1–28.
- (26) Hunkeler, W.; Möhler, H.; Pieri, L.; Polc, P.; Bonetti, E. P.; Cumin, R.; Schaffner, R.; Haefely, W. Selective Antagonists of Benzodiazepines. *Nature* **1981**, *290*, 514–515.
- (27) Jensen, L. H.; Petersen, E. N.; Braestrup, C.; Honoré, T.; Kehr, W.; Stephens, D. N.; Schneider, H.; Seidelmann, D.; Schmichen, R. Evaluation of the beta-Carboline ZK93426 as a Benzodiazepine Receptor Antagonist. *Psychopharmacology* **1984**, *83*, 249–256.
- (28) Valin, A.; Dodd, R. H.; Liston, D. R.; Potier, P.; Rossier, J. Methyl- β -Carboline-Induced Convulsions are Antagonized by Ro 15-1788 and by Propyl- β -Carboline. *Eur. J. Pharmacol.* **1982**, *85*, 93–97.
- (29) Cox, E. D.; Hagen, T. J.; McKernan, R. M.; Cook, J. M. BZ1 Receptor Subtype Specific Ligands. Synthesis and Biological Properties of BCC1, a BZ1 Subtype Specific Antagonist. *Med. Chem. Res.* **1995**, *5*, 710–718.
- (30) Fryer, R. I. In *Comprehensive Medicinal Chemistry*; Hansch, C., Sammes, P. G., Taylor, J. B., Eds; Pergamon: Oxford, 1990, Vol. 3, pp 539–566.
- (31) Da Settimo, A.; Primofiore, G.; Da Settimo, F.; Marini, A. M.; Novellino, E.; Greco, G.; Martini, C.; Giannaccini, G.; Lucacchini, A. Synthesis, Structure–Activity Relationships and Molecular Modeling Studies of *N*-(Indol-3-ylglyoxylyl)benzylamine Derivatives Acting at the Benzodiazepine Receptor. *J. Med. Chem.* **1996**, *39*, 5083–5091.
- (32) Primofiore, G.; Da Settimo, F.; Taliani, S.; Marini, A. M.; Novellino, E.; Greco, G.; La Vecchia, A.; Besnard, F.; Trincavelli, L.; Costa, B.; Martini, C. Novel *N*-(Arylalkyl)indol-3-ylglyoxylamides Targeted as Ligands of the Benzodiazepine Receptor: Synthesis, Biological Evaluation and Molecular Modeling Analysis of the Structure–Activity Relationships. *J. Med. Chem.* **2001**, *44*, 2286–2297.
- (33) Fryer, R. I.; Zhang, P.; Rios, R. The Synthesis of Substituted 2-Aminophenyl Heterocyclic Ketones. *Synth. Commun.* **1993**, *23*, 985–992.
- (34) Fryer, R. I.; Gu, Z. Q.; Wang, C. G. Synthesis of Novel, Substituted 4*H*-Imidazo[1,5-*a*][1,4]benzodiazepine. *J. Heterocycl. Chem.* **1991**, *28*, 1661–1669.
- (35) Hall, J. H.; Behr, F. E.; Reed, R. L. Cyclization of 2-Azidobenzophenones to 3-Phenylanthranyls. An Example of an Intramolecular 1,3-Dipolar Addition. *J. Am. Chem. Soc.* **1972**, *94*, 4952–4958.
- (36) Cappelli, A.; Anzini, M.; Vomero, S.; Canullo, L.; Mennuni, L.; Makovec, F.; Doucet, E.; Hamon, M.; Menziani, M. C.; De Benedetti, P. G.; Bruni, G.; Romeo, M. R.; Donati, S. Novel Potent and Selective 5-HT₃ Receptor Ligands Provided with Different Intrinsic Efficacy. 2. Molecular Basis of the Intrinsic Efficacy of Arylpiperazine Derivatives at the 5-HT₃ Receptors. *J. Med. Chem.* **1999**, *42*, 1556–1575.
- (37) Braestrup, C.; Nielsen, M. Benzodiazepine Receptors. In *Handbook of Psychopharmacology*; Iversen, L. L., Iversen, S. D., Snyder, S. H., Eds.; Plenum Press: New York, 1983, Vol. 17, pp 285–384.
- (38) Fryer, R. I.; Rios, R.; Zhang, P.; Gu, Z. Q.; Basile, A. S.; Skolnick, P. Structure–Activity relationships of 2-Pyrazolo[4,3-*c*]quinoline-3-ones and their *N*- and *O*-Methyl Analogues at Benzodiazepine Receptors. *Med. Chem. Res.* **1993**, *3*, 122–130.
- (39) Razzugin, A. V.; Mecozzi, S. Binding Properties of Aromatic Carbon-Bound Fluorine. *J. Med. Chem.* **2006**, *49*, 7902–7906.
- (40) Schwartz, R. D.; Suzdak, P. D.; Paul, S. M. α -Aminobutyric Acid (GABA)- and Barbiturate-Mediated ³⁶Cl[−] Uptake in Rat Brain Synaptosomes: Evidence for Rapid Desensitization of the GABA Receptor-Coupled Chloride Ion Channel. *Mol. Pharmacol.* **1986**, *30*, 419–426.
- (41) Im, H. K.; Im, W. B.; Hamilton, B. J.; Carter, D. B.; VonVoigtlander, P. F. Potentiation of GABA-Induced Chloride Currents by Various Benzodiazepine Site Agonists with $\alpha_1\gamma_2\beta_2\gamma_2$ and $\alpha_1\beta_2\gamma_2$ Subtypes of Cloned GABA_A Receptors. *Mol. Pharmacol.* **1993**, *44*, 866–870.
- (42) *tert*-Butyl 5-Acetyl-4,5-dihydroimidazo[1,5-*a*]quinoxaline-3-carboxylate is reported as compound **13h** in the paper by TenBrink, R. E.; Im, W. B.; Sethy, V. H.; Tang, A. H.; Carter, D. B. Antagonist, Partial Agonist, and Full Agonist Imidazo[1,5-*a*]quinoxaline Amides and Carbamates Acting through GABA_A/Benzodiazepine Receptor. *J. Med. Chem.* **1994**, *37*, 758–768. This compound was re-synthesized according to the published procedure and its spectral and analytical data were consistent with those reported therein.
- (43) Kloda, J. H.; Czajkowski, C. Agonist-, Antagonist-, and Benzodiazepine-Induced Structural Changes in the [alpha]1 Met113-Leu132 Region of the GABAA Receptor. *Mol. Pharmacol.* **2007**, *71*, 483–493.
- (44) Campo-Soria, C.; Chang, Y.; Weiss, D. S. Mechanism of Action of Benzodiazepines on GABA_A Receptors. *Br. J. Pharmacol.* **2006**, *148*, 984–990.
- (45) Jones-Davis, D. M.; Song, L.; Gallagher, M. J.; MacDonald, R. L. Structural Determinants of Benzodiazepine Allosteric Regulation of GABA_A Receptor Currents. *J. Neurosci.* **2005**, *25*, 8056–8065.
- (46) Lopez-Romero, B.; Evrard, G.; Durant, F.; Sevrin, M.; P. George Molecular Structure and Stereoelectronic Properties of Sarmazenil a Weak Inverse Agonist at the Omega Modulatory Sites (Benzodiazepine Receptors): Comparison with Bretazenil and Flumazenil. *Bioorg. Med. Chem.* **1998**, *6*, 1745–1757.
- (47) Fryer, R. I.; Cook, C.; Gilman, N. W.; Walser, A. Conformational Shift at Benzodiazepine Receptor Related to the Binding of Agonist, Antagonists and Inverse Agonists. *Life Sci.* **1986**, *39*, 1947–1957.
- (48) Shove, L. T.; Perez, J. J.; Loew, G. H. Molecular Determinants of Recognition and Activation at Cerebellar Benzodiazepine Receptor Site. *Bioorg. Med. Chem.* **1994**, *2*, 1029–1049.
- (49) Clayton, T.; Chen, J. L.; Ernst, M.; Richter, L.; Cromer, B. A.; Morton, C. J.; Ng, H.; Kaczorowski, C. C.; Helmstetter, F. J.; Furtmuller, R.; Ecker, G.; Parker, M. W.; Sieghart, W.; Cook, J. M. An updated unified pharmacophore model of the benzodiazepine binding site on γ -aminobutyric acid receptors: correlation with comparative models. *Curr. Med. Chem.* **2007**, *14*, 2755–2775.
- (50) Cromer, B. A.; Morton, J. C.; Parker, M. W. Anxiety over GABA_A Receptor Structure Relieved by AChBP. *Trends Biochem. Sci.* **2002**, *27*, 280–287.
- (51) Lam, P. C.-H.; Carlier, P. R. Experimental and Computational Studies of Ring Inversion of 1,4-Benzodiazepine-2-ones: Implications for Memory of Chirality Transformations. *J. Org. Chem.* **2005**, *70*, 1530–1538.
- (52) Morris, G. M.; Goodsell, D. S.; Halliday, R. S.; Huey, R.; Hart, W. E.; Belew, R. K.; Olson, A. J. Automated Docking Using a Lamarckian Genetic Algorithm and Empirical Binding Free Energy Function. *J. Comput. Chem.* **1998**, *19*, 1639–1662.
- (53) Sigel, E.; Buhr, A. The Benzodiazepines Binding Site of GABA_A Receptor. *Trends Pharmacol. Sci.* **1997**, *18*, 425–429.
- (54) Mihic, S. J.; Withing, P. J.; Klein, R. L.; Wafford, K. A.; Harris, R. A. A Single Aminoacid of the Human γ -Aminobutyric Acid Type A Receptor γ_2 Subunit Determines Benzodiazepine Efficacy. *J. Biol. Chem.* **1994**, *269*, 32768–32773.
- (55) Wieland, H. A.; Luddens, H.; Seeburg, P. H. A Single Histidine in GABA_A Receptors is Essential for Benzodiazepine Agonist Binding. *J. Biol. Chem.* **1992**, *267*, 1426–1429.
- (56) Sigel, E.; Schaefer, M. T.; Buhr, A.; Baur, R. The Benzodiazepine Binding Pocket of Recombinant $\alpha_1\beta_2\gamma_2$ γ -Aminobutyric Acid_A receptors: Relative Orientation of Ligands and Amino Acid Side Chains. *Mol. Pharmacol.* **1998**, *54*, 1097–1105.
- (57) Tan, K. R.; Baur, R.; Gonther, A.; Goeldner, M.; Siegel, E. Two neighboring residues of loop A of the α_1 subunit point towards the benzodiazepine binding site of GABA_A receptor. *FEBS Lett.* **2007**, *581*, 4718–4722.

- (58) Primofiore, G.; Da Settimo, F.; Taliani, S.; Marini, A. M.; Novellino, E.; Greco, G.; Lavecchia, A.; Besnard, F.; Trincavelli, L.; Costa, B.; Martini, C. Novel *N*-(Arylalkyl)indol-3-ylglyoxylylamides Targeted as Ligand of the Benzodiazepine Receptor: Synthesis, Biological Evaluation, and Molecular Modeling Analysis of the Structure–Activity Relationships. *J. Med. Chem.* **2001**, *44*, 2286–2297.
- (59) Kucken, A. M.; Teissière, J. A.; Seffinga-Clark, J.; Wagner, D. A.; Czajkowski, C. Structural Requirements for Imidazobenzodiazepine Binding to GABAA Receptors. *Mol. Pharmacol.* **2003**, *63*, 289–296.
- (60) Kofron, W. G.; Baclawski, L. A Convenient Method for Estimation of Alkyl Lithium Concentrations. *J. Org. Chem.* **1976**, *41*, 1879–1880.
- (61) Walsh, D. A. The Synthesis of 2-Aminobenzophenones. *Synthesis* **1980**, *32*, 677–688.
- (62) Sheldrick, G. M. *SHELXS-97, Release 97-2, A Program for Automatic Solution of Crystal Structures*; Göttingen University: Göttingen, Germany, 1997.
- (63) Sheldrick, G. M. *SHELXL-97, Release 97-2, A Program for Crystal Structure Refinement*; Göttingen University: Göttingen, Germany, 1997.
- (64) Martini, C.; Lucacchini, A.; Ronca, G.; Hrelia, S.; Rossi, C. A. Isolation of Putative Benzodiazepine Receptors from Rat Brain Membranes by Affinity Chromatography. *J. Neurochem.* **1982**, *38*, 15–19.
- (65) Martini, C.; Rigacci, T.; Lucacchini, A. [³H]muscimol Binding Site on Purified Benzodiazepine Receptor. *J. Neurochem.* **1983**, *41*, 1183–1185.
- (66) Lowry, O. H.; Rosenbrouh, N. J.; Farr, A. L.; Randall, R. J. Protein Measurement with the Folin Phenol Reagent. *J. Biol. Chem.* **1951**, *193*, 265–275.
- (67) Bertelli, L.; Biagi, G.; Giorgi, I.; Manera, C.; Livi, O.; Scartoni, V.; Betti, L.; Giannaccini, G.; Trincavelli, L.; Barili, P. L. 1,2,3-Triazolo[1,5-*a*]quinoxalines: Synthesis and Binding to Benzodiazepine and Adenosine Receptors. *Eur. J. Med. Chem.* **1998**, *33*, 113–122.
- (68) Cheng, Y. C.; Prusoff, W. H. Relationship Between the Inhibition Constant (K_i) and the Concentration of Inhibition which Causes 50% Inhibition (IC_{50}) of an Enzyme Reaction. *Biochem. Pharmacol.* **1973**, *22*, 3099–3108.
- (69) Schwartz, R. D.; Suzdak, P. D.; Paul, S. M. γ -Aminobutyric Acid (GABA)- and Barbiturate-Mediated ³⁶Cl[−] Uptake in Rat Brain Synaptoneurosome: Evidence for Rapid Desensitization of the GABA Receptor-Coupled Chloride Ion Channel. *Mol. Pharmacol.* **1986**, *30*, 419–426.
- (70) Vaught, J.; Pelley, K.; Costa, L. G.; Setler, P.; Enna, S. J. A Comparison of the Antinociceptive Responses to GABA-receptor agonist THIP and Baclofen. *Neuropharmacology* **1985**, *4*, 211–216.
- (71) Walsh, D. M.; Stratton, S. C.; Harvey, F. J.; Beresford, I. J.; Hagan, R. M. The Anxiolytic-Like Activity of GR159897, a Non-Peptide NK2 Receptor Antagonist, in Rodent and Primate Models of Anxiety. *Psychopharmacology* **1995**, *122*, 186–191.
- (72) Malcangio, M.; Bartolini, A.; Ghelardini, C.; Bernardini, F.; Malmberg-Aiello, P.; Franconi, F.; Giotti, A. Effect of ICV Taurine on the Impairment of Learning, Convulsions and Death Caused by Hypoxia. *Psychopharmacology* **1989**, *98*, 316–320.
- (73) Jarvik, M. E.; Kopp, R. An Improved One-Trial Passive Avoidance Learning Situation. *Psychol. Rep.*, **1967**, *21*, 221–224.
- (74) Brooks, B. R.; Brucoleri, R. E.; Olafson, D.; States, D. J.; Swaminathan, S.; Karplus, M. CHARMM: A Program for Macromolecular Energy, Minimization and Dynamics Calculations. *J. Comput. Chem.* **1993**, *4*, 187–217.
- (75) Gasteiger, J.; Marsili, M. Iterative Partial Equalization of Orbital Electronegativity—A Rapid Access to Atomic Charges. *Tetrahedron* **1980**, *36*, 3219–3228.
- (76) Phillips, J. C.; Braun, R.; Wang, W.; Gumbart, J.; Tajkhorshid, E.; Villa, E.; Chipot, C.; Skeel, R. D.; Kale, L.; Schulten, K. Scalable Molecular Dynamics with NAMD. *J. Comput. Chem.* **2005**, *26*, 1781–1802.
- (77) Case, D. A.; Darden, T. A.; Cheatham, T. E.; Simmerling, C. L.; Wang, J.; Duke, R. E.; Luo, R.; Merz, K. M.; Pearlman, D. A.; Crowley, M.; Walker, R. C.; Zhang, W.; Wang, B.; Hayik, S.; Roitberg, A.; Seabra, G.; Wong, K. F.; Paesani, F.; Wu, X.; Brozell, S.; Tsui, V.; Gohlke, H.; Yang, L.; Tan, C.; Mongan, J.; Hornak, V.; Cui, G.; Beroza, P.; Matthews, D. H.; Schafmeister, C.; Ross, W. S.; Kollman, P. A. *AMBER 9*; University of California: San Francisco, 2006.
- (78) Wang, J.; Cieplak, P.; P.A. Kollman. How Well Does a Restrained Electrostatic Potential (RESP) Model Perform in Calculating Conformational Energies of Organic and Biological Molecules. *J. Comput. Chem.* **2000**, *21*, 1049–1074.
- (79) Cornell, W. D.; Cieplak, P.; Bayly, C. I.; Gould, I. R.; Merz, K. M.; Ferguson, D. M.; Spellmeyer, D. C.; Fox, T.; Caldwell, J. W.; Kollman, P. A. A Second Generation Force Field for the Simulation of Proteins, Nucleic Acids, and Organic Molecules. *J. Am. Chem. Soc.* **1995**, *117*, 5179–5197.
- (80) Jorgensen, W. L.; Chandrasekhar, J.; Madura, J. D.; Impey, R. W.; Klein, L. M. Comparison of Simple Potential Functions for Simulating Liquid Water. *J. Chem. Phys.* **1983**, *79*, 926–935.
- (81) Martyna, G. J.; Tobias, D. J.; Klein, M. L. Constant Pressure Molecular Dynamics Algorithms. *J. Chem. Phys.* **1994**, *101*, 4177–4189.
- (82) Essmann, U.; Perera, L.; Berkowitz, M. L.; Darden, T.; Lee, H.; Pedersen, L. G. A Smooth Particle Mesh Ewald Method. *J. Chem. Phys.* **1995**, *103*, 8577–8593.
- (83) Ryckaert, J.-P.; Ciccotti, G.; Berendsen, H. J. C. Numerical Integration of the Cartesian Equations of Motion of a System with Constraints: Molecular Dynamics of *n*-Alkanes. *J. Comput. Phys.* **1977**, *23*, 327–341.
- (84) Humphrey, W.; Dalke, A.; Schulten, K. VMD: Visual Molecular Dynamics. *J. Mol. Graphics* **1996**, *14*, 33–38.

JM8002944